Copyright Warning & Restrictions

The copyright law of the United States (Title 17, United States Code) governs the making of photocopies or other reproductions of copyrighted material.

Under certain conditions specified in the law, libraries and archives are authorized to furnish a photocopy or other reproduction. One of these specified conditions is that the photocopy or reproduction is not to be "used for any purpose other than private study, scholarship, or research." If a, user makes a request for, or later uses, a photocopy or reproduction for purposes in excess of "fair use" that user may be liable for copyright infringement,

This institution reserves the right to refuse to accept a copying order if, in its judgment, fulfillment of the order would involve violation of copyright law.

Please Note: The author retains the copyright while the New Jersey Institute of Technology reserves the right to distribute this thesis or dissertation

Printing note: If you do not wish to print this page, then select "Pages from: first page # to: last page #" on the print dialog screen

ABSTRACT

OPTIMIZATION OF THE FRONT END OF CDTE SOLAR CELLS

by
Yunfei Chen

The front end of CdTe solar cells consists of two layers: a transparent conducting oxide (TCO) layer and a window layer. New wider band gap materials, ZnMgO are being used to replace CdS as the window layer for the purpose of removing blue loss. For ZnMgO, three important parameters, including the atomic Mg content (*x*), thickness (*t*), and doping concentration (*n*) can play important roles on the performance of CdTe solar cells. In this dissertation, systematic simulation, by solar cell capacitance simulator (SCAPS), and experiments are used to investigate the influences of these parameters on the performance of CdTe solar cells.

The optimized parameters of the window layer are found as follows: 10% atomic Mg content to adjust the value of conduction band offset at 0.3 eV. 40 nm thickness with 10^{18} cm^{-3} doping concentration to form an n^{+}-p junction structure with the p-type CdTe absorber. Besides, the optimized thickness of different types of TCO is also theoretical calculated. Some novel ideas have been proposed and discussed, but may not be able to enhance the performance of CdTe solar cells.

OPTIMIZATION OF THE FRONT END OF CDTE SOLAR CELLS

by
Yunfei Chen

A Dissertation
Submitted to the Faculty of
New Jersey Institute of Technology
in Partial Fulfillment of the Requirements for the Degree of
Doctor of Philosophy in Materials Science and Engineering

Program of Materials Science and Engineering
CNBM New Energy Materials Research Center, NJIT

December 2017

.

APPROVAL PAGE

OPTIMIZATION OF THE FRONT END OF CDTE SOLAR CELLS

Yunfei Chen

Dr. Ken K. Chin, Advisor — Date
Professor of Physics, NJIT

Dr. Alan E. Delahoy, Committee Member — Date
Research Professor of Physics, NJIT

Dr. N. M. Ravindra, Committee Member — Date
Professor of Physics, NJIT

Dr. Dong-Kyun Ko, Committee Member — Date
Assistant Professor of Electrical and Computer Engineering, NJIT

Dr. Yong Yan, Committee Member — Date
Assistant Professor of Chemistry, NJIT

BIOGRAPHICAL SKETCH

Author: Yunfei Chen

Degree: Doctor of Philosophy

Date: December 2017

Undergraduate and Graduate Education:

- Doctor of Philosophy in Materials Engineering,
  New Jersey Institute of Technology, Newark, NJ, 2017

- Master of Science in Materials Science and Engineering,
  New Jersey Institute of Technology, Newark, NJ, 2013

- Bachelor of Science in Materials Science and Engineering,
  Hunan University, Changsha, Hunan, P. R. China, 2011

Major: Materials Science and Engineering

Presentations and Publications:

Y. Chen, S. Peng, X. Tan, X. Cao, B. Siepchen, G. Fu, A. Delahoy, and K. Chin, in Proceedings of IEEE PVSC (2016), pp. 424–427.

Y. Chen, S. Peng, X. Cao, A. Delahoy, and K. Chin, in Proceedings of IEEE Photovoltaic Specialist Conference (2017).

Y. Chen, X. Tan, S. Peng, C. Xin, A. Delahoy, K. Chin, and C. Zhang, J. Electron. Mater. (2017), https://doi.org/10.1007/s11664-017-5850-9.

This thesis is dedicated to all the persons who help me during my years of pursuing the degree of Ph.D, especially my loving parents and my advisor Dr. Ken K. Chin.

ACKNOWLEDGMENT

I wish to thank all my committee members for their time, energy and effort they have paid on this dissertation. A special thanks to Dr. Ken K. Chin, my Advisor, who is always energetic with new ideas and ready to answer my questions. His knowledge and experience on the research topic was really helpful during my PhD study. Also a special thanks to Dr. Alan E. Delahoy who consistently provided help during my PhD study, especially for his experimental expertise in ZMO preparation and for elucidating the concepts needed to understand the TCO/metal oxide/absorber type solar cell. Thanks you Dr N.M Ravindra, Dr. Dong-kyun Ko, and Dr. Yong Yan, who was serving on my Committee, and also making valuable suggestions on the thesis manuscript.

I would like to acknowledge Chinese National Building Material Company who paid for my Research Assistantship and the financial support to our center. Special thanks to Professor Kevin Belfield, Dean of College of Science and Liberal Arts, who awarded me Teaching Assistantship.

Finally, I would like to thank Dr. Zimeng Cheng who brought me into the CdTe solar cells area, Dr. Xuehai Tan who taught me valuable lab skills and writing techniques, and Dr. Chuanjun Zhang who helped a lot during the end of my studies. My sincere thanks also go to our center's workers, Payal and Akash, who provided me some of the experimental data.

TABLE OF CONTENTS

Chapter		Page
1	INTRODUCTION	1
	1.1 Objective	1
	1.2 Background Information	2
	1.2.1 Thin Film Solar Cells	2
	1.2.2 CdTe Solar Cells	3
	1.3 Window Layer of CdTe Solar Cells	7
	1.3.1 Materials the Window Layer	7
	1.3.2 Important Parameters of the Window Layer	12
	1.4 TCO Layer of CdTe Solar Cells	20
2	SIMULATION METHOD	22
3	EXPERIMENTAL METHOD	27
	3.1 Processing of the CdTe Solar Cell	27
	3.1.1 TCO	27
	3.1.2 ZnMgO	27
	3.1.3 CdS	28
	3.1.4 CdTe	31
	3.1.5 Cu	35
	3.2 Characterization Methods of ZnMgO and CdTe Solar cell	36
	3.2.1 Characterization of ZnMgO	36
	3.2.2 C haracterization of CdTe Solar Cells	37

TABLE OF CONTENTS
(Continued)

Chapter		Page
4	THE INFLUENCE OF Mg CONTENT	39
	4.1 Theoretical Analysis	39
	4.2 Simulated Results	48
	4.3 Experimental Results	56
5	THE INFLUENCE OF THICKNESS & DOPING CONCENTRATION	61
	5.1 Theoretical Analysis	61
	5.2 Simulated Results	64
	5.3 Experimental Results	76
6	THE INFLUENCE OF TCO LAYER	81
7	CONCLUSION	86
	7.1 Some Novel Ideas on the Front End	86
	7.2 Conclusions on the Front End	89
REFERENCES		92

LIST OF TABLES

Table		Page
1.1	The Efficiency of Different Thin Film Solar Cells	3
1.2	Band Gap of CdSO Samples Deposited at Different O_2/Ar Ratios	8
2.1	Initial Input Parameters of Each Component in the Simulation	24
5.1	Conditions to Determine the Structure of CdTe Solar Cells	62
5.2	The influence of the Thickness of ZnMgO at Different Structure of CdTe Solar Cells from the Simulated Results	69
5.3	The Measured J-V Results for CdTe Solar Cells with Different Thickness of ZnMgO.	77
5.4	The Hall Measurement Results of the Deposited ZnMgO Samples	78
6.1	The Measured Optical and Electrical Properties of the TCO Samples.	83
7.1	Performance Comparison of CdTe Cells Processed at CNBM Center and CSU	90
7.2	The Concluded Optimized Parameters of the Window Layer for CdTe Solar Cells	91

LIST OF FIGURES

Figure **Page**

1.1 A typical structure of CdTe solar cell. 4

1.2 The J-V performance of the CdTe solar cells with different O_2/Ar ratios during CdSO deposition..... 9

1.3 Electron affinity of ZnMgO as function of n. 10

1.4 J-V curve of the CdTe solar cell from CSU using ZnMgO as the window layer with an efficiency of 18.3%. 11

1.5 J-V curves of our center's CdTE solar cell using TMO as the window layer under both light and dark conditions. 12

1.6 Measured QE results of CdTe solar cells from CSU using CdS and CdSO as the window layer, respectively. 13

1.7 Measured QE results of CdTe solar cells from CSU using Ga-doped ZMO as the window layer. 14

1.8 Simulated J-V results of CdTe solar cells from CSU with different values of conduction band offset..... 15

1.9 Contribution to short-circuit current from photons with energy greater than the CdS bandgap as a function of CdS thickness..... 17

1.10 J-V performances of CdTe solar cells as a function of CdS layer thickness..... 17

1.11 Measured J-V results of CdTe solar cells with different Mg content and thickness of ZnMgO layer from CSU. 18

2.1 The structure of simulated CdTe solar cell. 23

3.1 The water bath station for CBD. 29

3.2 The photograph and description of the self-designed small CSS equipment in our lab. 32

3.3 Schematic diagram for CSS process. 33

3.4 The optical properties of the measured CdSO samples. 37

LIST OF FIGURES
(Continued)

Figure **Page**

4.1 Flat band diagrams of CdTe solar cells..... 43

4.2 The calculated thermionic emission current density..... 45

4.3 Schematic diagram of the intra-band tunneling mechanism..... 46

4.4 The calculated net current density crossing the interface as a function of conduction band offset..... 47

4.5 Simulated results of CdTe solar cells with different materials as the window layer..... 49

4.6 Simulated performance of CdTe solar cell as a function of ΔEC..... 51

4.7 Simulated band diagram of CdTe solar cells at different ΔEC with band bending enlarged..... 52

4.8 Simulated recombination rate near the interface areas. 53

4.9 Open-circuit voltage as a function of conduction band offset at different interface defect density. 54

4.10 QE measurement results of the fabricated CdTe solar cells using different kinds of window layer materials..... 57

4.11 J-V measurement results of the fabricated CdTe solar cell using HCS ZnMgO as the window layer..... 58

4.12 J-V results of CdTe solar cells using ZnMgO with 15% atomic Mg content and 12% atomic Mg content, respectively, as the window layer..... 59

5.1 Simulated QE results on two different thickness of ZnMgO..... 65

5.2 Simulated QE results on two different thicknesses of CdS. 65

5.3 J-V performance of CdTe solar cells as a function of the thickness at different doping concentrations of ZnMgO. 68

5.4 J-V performance of CdTe solar cells as a function of the doping concentraion at different thicknesses of ZnMgO..... 72

LIST OF FIGURES
(Continued)

Figure **Page**

5.5 J-V performance of the simulated CdTe solar cell with different doping concentration of ZnMgO..... 74

5.6 Conduction band diagram of the simulated CdTe solar cells. 75

5.7 The measured J-V curves of CdTe solar cells with different thickness of ZnMgO..... 78

5.8 Measured J-V performance of CdTe solar cells with different doping concentration of ZnMgO..... 80

6.1 The schematic diagram of the current in the TCO layer of the solar cell module..... 84

7.1 Simulated J-V results with different structures and different conduction band offset for CdTe solar cells. 87

7.2 The conduction band diagram of the simulated CdTe solar cells with two ZnMgO layers. 88

CHAPTER 1

INTRODUCTION

1.1 Objective

The objective of this dissertation is to find out the optimized front end of CdTe solar cells. The front end of CdTe usually consists of two layers, a TCO layer and a window layer. ZnMgO is the material used in this dissertation to optimize the window layer. For ZnMgO, three parameters, including atomic Mg content (x), thickness (t) and doping concentration (n) are specifically discussed. The influence of these three parameters on the performance of CdTe solar cells were provided by both simulated and experimental results. The optimization of the thickness for the TCO layer is also theoretically calculated. Typically, it is TCO with SnO_2 buffer that is used in the fabrication of CdTe solar cells as well as modules. In this thesis, we do not include this layer. Its role in the CdTe solar cell is similar to that of the undoped or low doped ZMO.

For the simulation part, computer software called SCAPS (a Solar Cell Capacitance Simulator) is used to simulate the influence of the three parameters of ZnMgO layer on the performance of CdTe solar cells.

For the experimental part, we used the solar cell processing and characterization equipment of the CNBM New Energy Materials Research Center, NJIT. We list and discuss the relevant facilities in the dissertation. Different characterization methods on both the deposited ZnMgO layer and the fabricated CdTe solar cells are introduced to investigate the influence of the three parameters on the performance of CdTe solar cells.

The simulated results are compared with the experimental results and deep discussion of the results is included.

1.2 Background Information

1.2.1 Thin Film Solar Cells

Thin film solar cells are second generation photovoltaic (PV) devices. As the word 'thin film' means, they consist of different thin film layers or thin film of photovoltaic absorber layer on a substrate (superstrate), for example glass. The current three main branches of thin film solar cells are amorphous silicon solar cells, CdTe solar cells and CIGS solar cells.

Compared to the conventional, the first generation crystalline silicon solar cells, the thickness of the layers of CdTe solar cells are much thinner. This means thin film solar cells have advantages of less cost, less weight, less drag and more flexible than crystalline silicon solar cells. However, they are suffering the problems of lower efficiency and faster degradation than crystalline silicon solar cells. These problems limit the commercial applications of thin film solar cells. Actually, the market-share of thin film solar cells has been declining for the last 10 years. For the year of 2013, the market-share for amorphous silicon, CdTe, and CIGS panels are 2.0%, 5.1%, and 2.0%, respectively [1].

The potential of thin film solar cells' efficiency should be larger than 20% for the cell size and larger than 15% for production modules. The latest reported efficiency of the different thin film solar cells are listed in Table 1.1 [2].

Table 1.1 The Efficiency of Different Thin Film Solar Cells

Classification	**Efficiency** %	**Source**
Amorphous silicon (cell)	10.2±0.3	AIST
CdTe (cell)	21.0±0.4	First Solar
CIGS (cell)	21.0±0.6	Solibro
CIGS (minimodule)	18.7±0.6	Solibro

Source: M. Green, K. Emery, Y. Hishikawa, W. Warta, E. Dunlop, D. Levi, and A. Ho-Bailie, Prog. Photovolt: Res. Appl. 25, 3 (2017).

1.2.2 CdTe Solar Cells

CdTe solar cell is one of three main branches of the thin film solar cell. The room temperature (300K) band gap for CdTe is approximated 1.50 eV to 1.51 eV [3-5]. Modulated photo-reflectance is the most accurate way to measure it. For real CdTe solar cells, the band gap of CdTe can be lowered to 1.45 eV due to the formation of intermixing layer [6, 7]. Thus, the band gap of CdTe solar cell is ideal to yield high efficiency solar cell according to Shockley-Queisser diagram [8]. Before around 2011, A typical configuration of CdTe solar cell, as shown in Figure 1.1 [9], is comprised of a glass substrate, an indium tin oxide (ITO) layer as a transparent conductive oxide (TCO) layer playing a role as the front contact, a CdS layer serving a buffer to avoid direct contact between the TCO layer and CdTe layer, or serving as an electrode to form an n-p junction with CdTe so that the photo-generated carriers can be separated to lower down the recombination and increase carrier lifetime, a CdTe layer acting as the absorber and a Cu layer playing a role as the back contact. The TCO layer and the CdS layer can be defined as the front end whereas the CdTe and Cu layer can be defined as the absorber and the back contact back end of CdTe solar cells. Despite the great potential from the band gap of CdTe, the efficiency record of

CdTe solar cell with this structure was kept at only 16.5% until 2010 [10], which is far from the expected value from the Shockley-Queisser diagram.

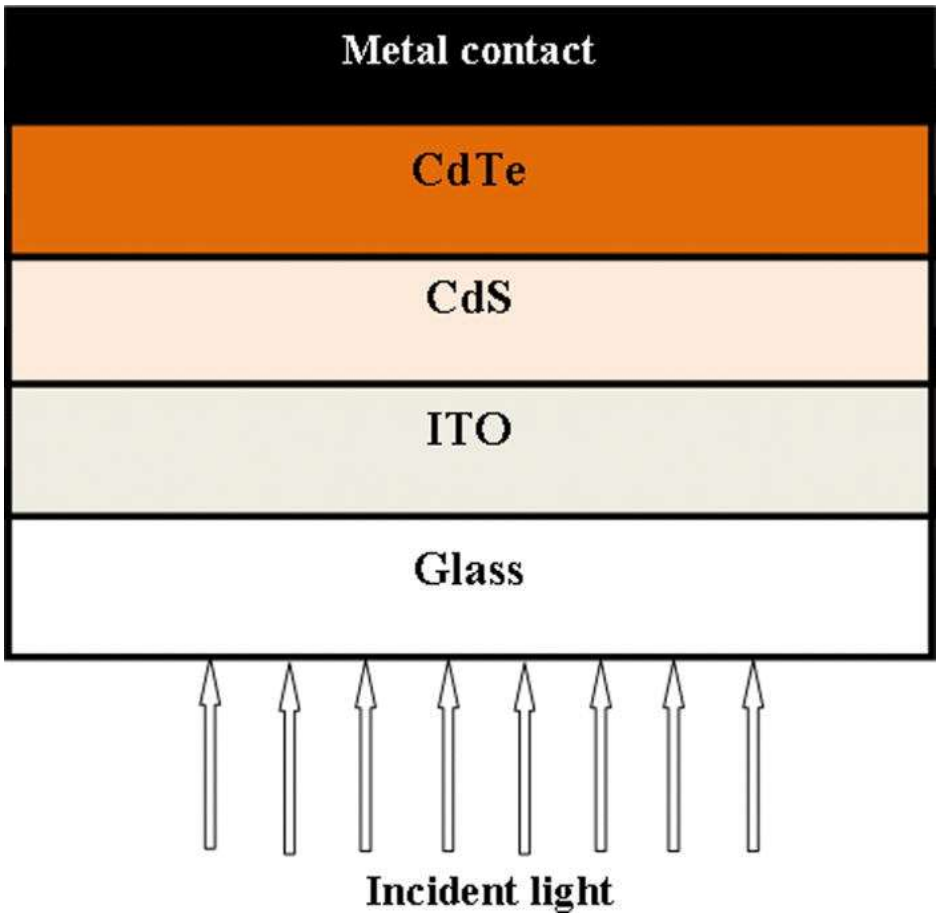

Figure 1.1 A typical structure of CdTe solar cell.

Source: A. Mohamed, J. Appl. Phys. 113, 093105 (2013).

There are two main limiting factors of this traditional structure of CdTe solar cells. First, the doping concentration of p-type CdTe is relatively low, usually at the order of 10^{14} cm^{-3} or 10^{15} cm^{-3}, which can prevent the enhancement of the open-circuit voltage, and short-circuit current of CdTe solar cells. Thus, modification on the CdTe absorber layer is required to improve the performance of CdTe solar cells. Different techniques have been

tried by some researches in order to solve this issue, such as doping Cu in Te-rich CdTe and doping P or As in Cd-rich CdTe [11-14]. Works from other scientists indicate that graded doping in CdTe absorber is also helpful to increase the efficiency of CdTe solar cells [15-17]. Also, there are researchers paying effort on making CdSe/CdTe solar cells [18-21]. One reason to do it is the CdTeSe intermixing layer has a narrower bang gap than CdTe due to the bowing effect, and is closer to the most optimized solar cell band gap as Shockley-Quiesser diagram shows. Another reason is Se diffusion into CdTe may passivate the deep levels located at the thin film polycrystalline's boundaries. Some other methods include higher temperature during the deposition [22, 23], variations in the stoichiometry of the junction region [24, 25] and so on.

The other serious limiting factor is the blue loss due to the relatively low band gap of CdS. With a band gap of 2.45 eV, light with wavelength smaller than blue light will be absorbed in CdS layer. However, light absorption is not desired in CdS layer since lifetime of the photo-generated carriers in this layer is extremely low. This means with a CdS layer, this portion of light with wavelength smaller than blue light cannot contribute to the quantum response, leading to a significant loss of quantum efficiency and short-circuit current. Theoretical analysis indicates that the short-circuit loss of CdTe solar cells from the blue loss can be 1.4 mA/cm^2. This number can even increase to more than 5 mA/cm^2 in commercial solar panels [26, 27]. To avoid the blue loss, two ways have been used. One is reducing the thickness of CdS so that light absorption in this layer can be significantly reduced. But reducing the thickness will sacrifice the uniformity of the CdS layer. The outcome of pinholes will further lead to the formation of localized TCO/CdTe junctions, bringing to the excessive shunting and the efficiency loss. Employing a high resistive

transparent (HRT) layer is a feasible method to prevent this effect and improve the characteristic of CdTe solar cells. ZnO has already been proved as a promising material for the HRT layer by different researchers [28-30]. Certain thickness is needed to avoid the ITO diffusion into CdS layer. However, the increasing thickness of ZnO will finally negatively influence the performance of CdTe solar cells. A proper explanation of this behavior is that light absorption is also increasing in the ZnO layer with a raising thickness. Another way to reduce the blue loss is replacing CdS with wider band gap materials. Once wider band gap materials are adopted, the incoming visible light can successfully go through it and reach the CdTe solar absorber layer. Then this layer can be named as window layer. For convenience, this layer will always be called 'window layer' in the later sections or chapters even when the material of it is CdS. The dramatic efficiency enhancement of CdTe solar cells in the last six to seven years from 16.5% to 22.1% mainly originates from this [1, 31]. This means that studying and utilizing wider band gap semiconductors as the window layer is the key for high-efficiency CdTe solar cells and it is worthy to be investigated. Specific introduction on this will be provided in the following section.

Besides the two main limiting factors, the improvement on the back contact of CdTe solar cells has also been mentioned in order to minimize the recombination at the interface. A Te-rich layer is beneficial [32]. It can be achieved either by selective etching or by deposition of a separate Te layer. Some new alloy materials, such as CdMgTe or CdZnTe, is being tried for the purpose of reflecting electrons from back contact and reducing the barrier to photo-generated current [33, 34].

1.3 Window Layer of CdTe Solar Cells

1.3.1 Materials of the Window Layer

CdS has been widely used as the window layer of CdTe solar cells in the last decades of years. The reason is probably that the lattice mismatch between CdS and CdTe is small so that a good property interface can be formed. However, due to the significant blue loss caused by CdS, this material is no longer regarded as a proper one for good performance CdTe solar cells. As mentioned in the previous sections, wider band gap materials have been adopted to replace CdS as the window layer. This brings out the dramatic efficiency improvement in the last six to seven years.

CdSO is one of the candidates to replace CdS as the window layer. The group led by Wu first introduced this material into CdTe thin film technology in the early 2000s [35]. They synthesized CdSO samples by carrying out deposition at different oxygen/argon (O/Ar) ratios. The band gap of CdSO samples could then be precisely controlled, shown in Table 1.2 and a series of CdTe solar cells with a structure of CTO/ZTO/CdSO/CdTe were fabricated. Their fabricated CdTe solar cell using CdSO as the window layer is much better than those using CdS as the window layer. In 2014, researchers from the Colorado School of Mines then concluded that amorphous CdSO layers with an optical band gap of 2.8 eV and 45% O result in the highest observed efficiency [36]. CdSO was deeply analyzed by a group in University of Nevada through a publication in 2015 [37]. The results showed that CdSO films were mainly comprised of CdS and $CdSO_4$, with small additions of an intermediate $CdSO_x$ (most likely sulfite) species. $CdSO_4$ is the preferred species when oxygen incorporation is increasing, whereas the content of the intermediate oxide species remains constant. Further investigation on CdSO was finished by a research group in

Colorado State University through a publication in 2015 [38]. They ascribed the increase of the band gap of CdSO to the alloying of high band gap sulfate and sulfite with CdS. Experimental results indicated that the optimized range for the ratio Ar/O2 during the deposition of CdSO was 1.5– 2.5%, as shown in Figure 1.2. Although applying CdSO is as the window layer can yield superior performance of CdTe solar cells, the stability issue of CdSO must be considered. Especially, it is easy to decompose during our center's high temperature close space sublimation (CSS) process. This issue has not been successfully addressed so far, which limits the use of CdSO in our center. Thus, CdSO is not chosen in the experimental part of this dissertation.

Table 1.2 Band Gap of CdSO Samples Deposited at Different O_2/Ar Ratios

Sample #	**O_2/Ar** %	**Band gap** *eV*
1	0	2.42
2	1	2.52
3	2	2.65
4	3	2.80
5	5	3.17

Source: X. Wu, R. Dhere, Y. Yan, I. Romero, Y. Zhang, J. Zhou, C. Dehart, A. Duba, C. Perkins, and B. To, in Proceedings of IEEE Photovoltaic Specialist Conference (2002), pp. 531–534.

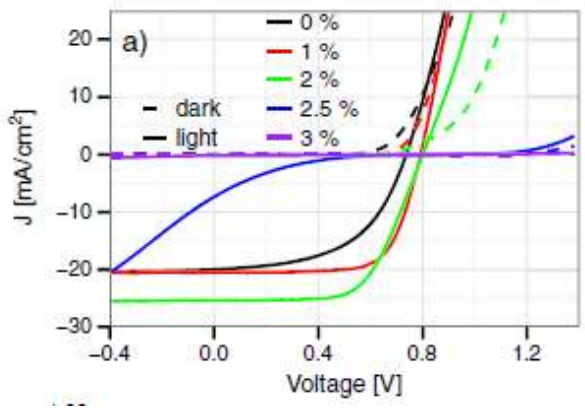

Figure 1.2 The J-V performance of the CdTe solar cells with different O_2/Ar ratios during CdSO deposition
Note: the higher O2/Ar ratio indicates higher O incorporation in the CdSO, resulting in wider band gap and, probably, larger conduction band offset in the CdSO window layer.
Source: J. Kephart, R. Geisthardt, and W. Sampath, Prog. Photovolt. Res. Appl. 123, 1484 (2015).

Besides CdSO, ZnMgO is also widely used as the window layer in different kinds of thin film solar cells. Takashi Minemoto first applied this material in the CIGS solar cells for the purpose of controlling conduction band offset between ZnMgO layer and CIGS layer. [39] Co-sputtering method of ZnO and MgO was used to deposit ZnMgO films. They found the ZMO band gap, as well as the conduction band offset between the ZnMgO/CIGS junction can be controlled by changing the Mg content in the deposited ZnMgO film. The band gap of ZnMgO should range from 3.3 eV, the band gap of ZnO, to 7.8 eV, the band gap of bulk MgO, or 6 to 6.5 eV [40, 41], the band gap of nanoscale ZnMgO, with the variation of Mg content. Unlike CdSO, no bowing effect was found for ZnMgO. The relationship between the band gap of ZnMgO with the Mg content was latter deeply investigated by other scientists. Maemoto's group showed a figure of the band gap of ZnMgO as a function of portion of MgO content in the ZnO + MgO content, shown in Figure 1.3 [42]. Specific relationship between the band gap of ZnMgO and the Mg content

has been set up by Lorenz et.al, as shown in Equation (1.1) when the x is smaller than 0.4 [43].

$$E_g(ZnMgO) = 3.296 + 2.19x \quad (1.1)$$

The influence of ZnMgO on the interface and bulk properties of CIGS solar cells was then investigated by Li et.al. They claimed that the ZnMgO/CIGS interface can reduce the concentration of holes in CIGS [44].

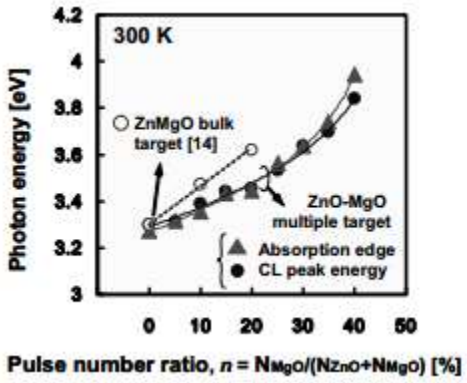

Figure 1.3 Electron affinity of ZnMgO as function of n.
Source: T. Maemono, N. Ichiba, H. Ishii, S. Sasa, and M. Inoue, J. Phys. Conf. Ser. 59, 670 (2007).

ZnMgO has been used for more than ten years. However, it is not until recently that ZnMgO is used in CdTe solar cells. This kind of research work was mostly reported by James Sites's group in Colorado State University [45-47]. They successfully made a CdTe solar cell with an efficiency of 18.3% with an increased open-circuit voltage and short-circuit current using a 100 nm ZnMgO as the window layer. The J-V curve of their solar cell is shown in Figure 1.4. Their later publication indicates that the efficiency of CdTe solar cells is possible to be raised to 24% if the back contact is improved. This promising result indicates that ZnMgO deserves further investigation. Thus, ZnMgO is

chosen as the material to investigate the influence of window layer on the performance of CdTe solar cells by both simulation and experimental methods.

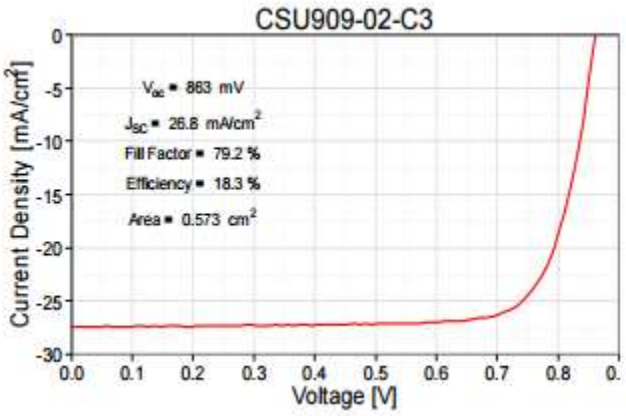

Figure 1.4 J-V curve of the CdTe solar cell from CSU using ZnMgO as the window layer with an efficiency of 18.3%.
Source: J. Sites, A. Munshi, J. Kephart. D. Swanson, and W. Sampath, in Proceedings of IEEE Photovoltaic Specialist Conference (2016), pp. 3632–3635.

Besides, our center's' recent publication reveals that using SnMgO (TMO), as the window layer, can also give a good performance for CdTe solar cells [48]. Although the short-circuit current and open-circuit voltage is a litter smaller than that made using ZnMgO as the window layer, the larger fill factor leads to a promising efficiency of 10.74%, which is the best record for our center's CdTe solar cells using wider band gap materials as window layers.

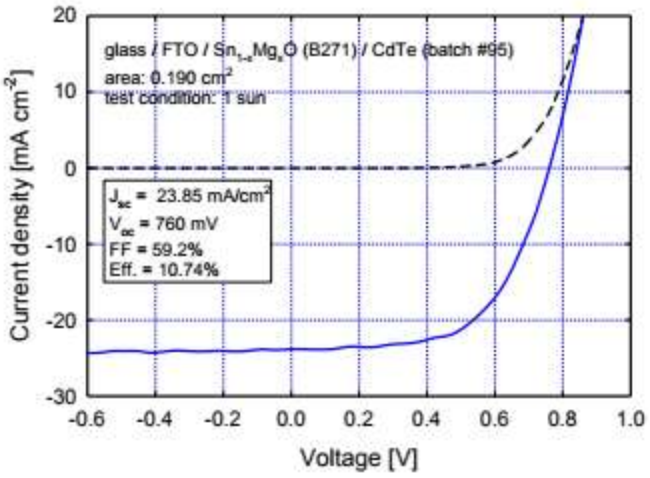

Figure 1.5 J-V curves of our center's CdTE solar cell using TMO as the window layer under both light and dark conditions.
Source: A. Delahoy, X. Tan, A. Saraf, P. Patra, S. Manda, Y. Chen, K. Velappan, B. Siepchen, S. Peng, and K. Chin, in Proceedings of IEEE Photovoltaic Specialist Conference (2017).

1.3.2 Important Parameters of the Window Layer

Four parameters of the window layer can significantly influence the properties of CdTe solar cells. These four parameters include band gap (E_g), electron affinity (χ), thickness (t), and doping concentration (n).

Band gap of the window layer has a strong influence on the performance of CdTe solar cells, as discussed above. When wider band gap materials are used as the window layer, the blue loss can be largely removed. Thus, the measured QE results using wider band gap materials as the window layer can be largely enhanced compared with that using traditional CdS as the window layer. Kephart et al. showed their QE results, shown in Figure 1.5, through a publication in 2011 IEEE Photovoltaic Specialist Conference (PVSC) [49]. The results proved that using CdSO as the window layer can increase the quantum efficiency of CdTe solar cells. Their later 2015 IEEE PVSC paper proves that using

ZnMgO (with Gallium-doped) as the TCO layer also can yield a good QE results as CdSO, as indicated in Figure 1.6 [50].

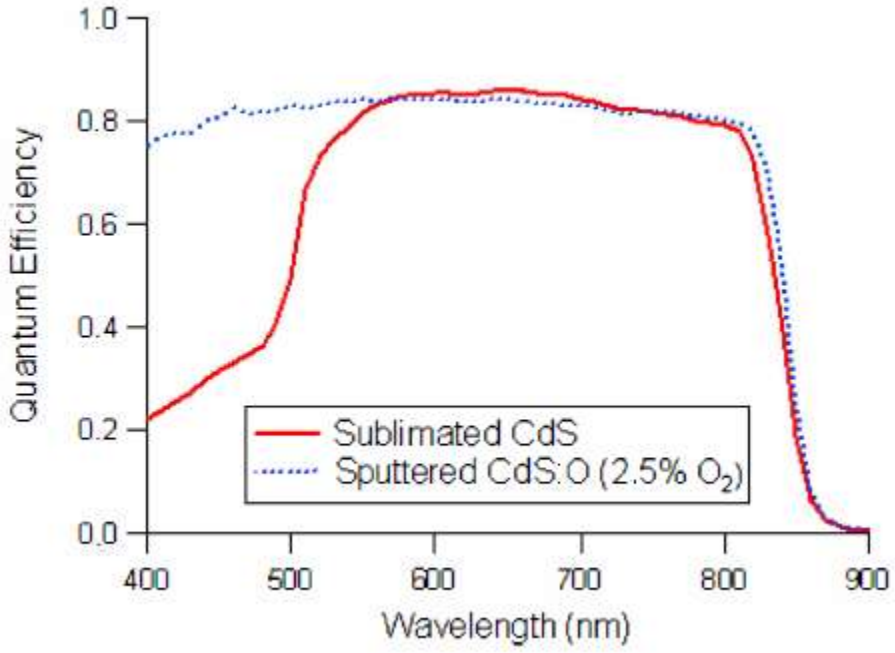

Figure 1.6 Measured QE results of CdTe solar cells from CSU using CdS and CdSO as the window layer, respectively.
Source: J. Kephart, R. Geisthardt, and S. Sampath, in Proceedings of IEEE Photovoltaic Specialist Conference (2011), pp. 854-858.

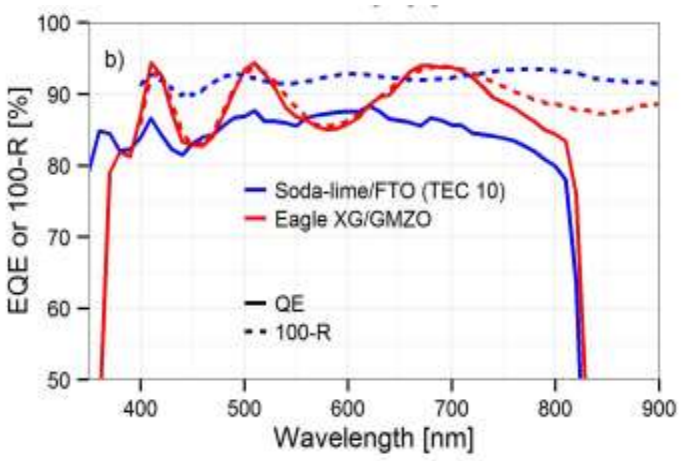

Figure 1.7 Measured QE results of CdTe solar cells from CSU using Ga-doped ZMO as the window layer.
Source: J. Kephart, and M. Sampath, in Proceedings of IEEE Photovoltaic Specialist Conference (2015), pp. 1-4.

The electron affinity of the window layer will mainly influence the conduction band offset (ΔE_C) between the window layer and the CdTe absorber layer. According to Anderson's rule, the conduction band offset between a heterojuction is determined by the two materials that form the heterojuction, as shown in Equation (1.2).

$$\Delta E_C = \chi_{absorber} - \chi_{window} \tag{1.2}$$

The influence of the conduction band offset and its optimized value or range has been investigated by some researchers through theoretical calculation and simulation. Minemoto's group first discussed the influence of the conduction band offset on the performance of CIGS solar cells. They reached a conclusion that the highest efficiency of CIGS solar cells can be achieved when the conduction band offset is in the range of 0 eV and 0.4 eV through their theoretical modeling [51]. The research group in CSU then briefly discussed the influence of the conduction band offset on the performance of CdTe solar cells through 1-D modeling [38]. The J-V curves of their simulated results at different

values of the conduction band offset were plotted, as shown in Figure 1.7. Their preliminary conclusion was that the optimized range of the conduction band offset should be 0.1 eV to 0.3 eV. In our previous work, deep theoretical analysis on the influence of conduction band offset was provided [52, 53] and a conduction band offset with a value of 0.2 eV or 0.3 eV was recommended. In this dissertation work, the simulated results and the theories in our previous work will be mentioned again but some improvements of the theories are inserted.

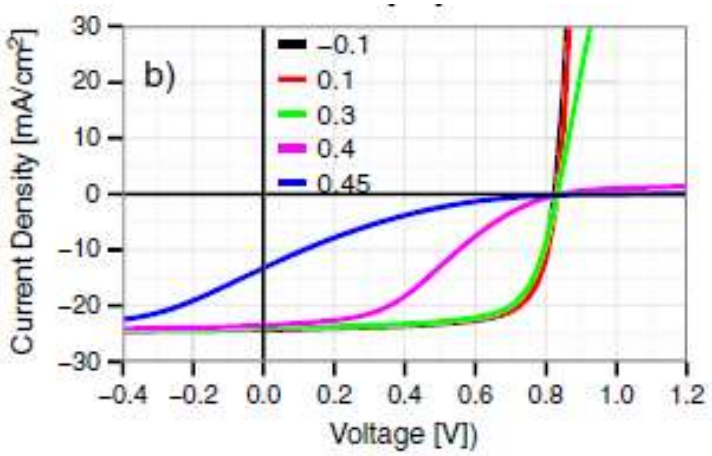

Figure 1.8 Simulated J-V results of CdTe solar cells from CSU with different values of conduction band offset.
*Note: The thickness and doping concentration of the window layer is 130 nm and 1*10^{16} cm^{-3}, respectively.*
Source: J. Kephart, R. Geisthardt, and W. Sampath, Prog. Photovolt. Res. Appl. 123, 1484 (2015).

The thickness of the window layer can influence the characteristics of CdTe solar cell. As mentioned above, when CdS is used as the window layer, reducing its thickness can largely avoid the blue loss. Thus, the short-circuit current is expected to enhance with the decrease of CdS's thickness. Figure 1.8 depicts the contribution of the incoming light with a wavelength smaller than the blue light's contribution to the final short-circuit current with the increasing thickness of CdS [54]. The results from other researchers' work

prove our guess. However, reducing the thickness of CdS does not mean that a higher efficiency of CdTe solar cells. Nakamura et al.'s paper found out that the open-circuit voltage and fill factor can drop significantly with the decrease of CdS's thickness, as shown in Figure 1.9 [55]. They argued that the decrease of CdS's thickness can lead to a decrease of the sulfur composition in the CdTeS intermixing layer and subsequently deteriorate the crystallinity of CdTe. The ascribed the dramatic decrease of open-circuit voltage of fill factor to the deterioration of the crystallinity of CdTe. When wider band gap material, such as CdSO or ZnMgO, is used, the blue loss issue does not have to be considered any more. But the thickness of the window may still influence the properties of CdTe solar cells. In Kephart et.al's paper published in 2016, the influence of the thickness of ZnMgO with different Mg content is plotted, as shown in Figure 1.10 [47]. They emphasized that for ZnMgO layer, the pinhole and lattice mismatch are not the key issues to yield a high efficiency CdTe solar cells. With higher magnesium, high open-circuit voltage can be achieved with thinner ZnMgO layers but fill factor is reduced due to a kink, in the J-V curve. A strong secondary barrier exists when the thickness of ZnMgO is higher than 100 nm, leading to a decrease in fill factor. The optimal point was achieved at 50 nm with 11 wt% MgO target.

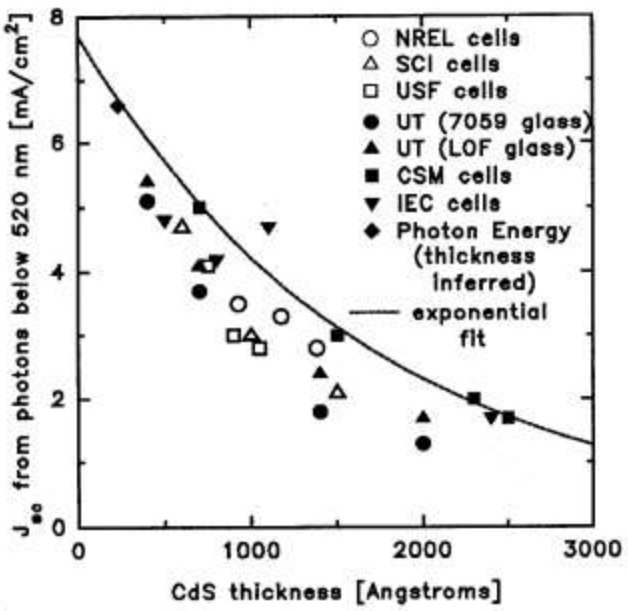

Figure 1.9 Contribution to short-circuit current from photons with energy greater than the CdS bandgap as a function of CdS thickness.
Source: J. Granata, J. Sites, G. Contreras-Puente, and A. Compaan, in Proceedings of IEEE Photovoltaic Specialist Conference (1996), pp. 854-856.

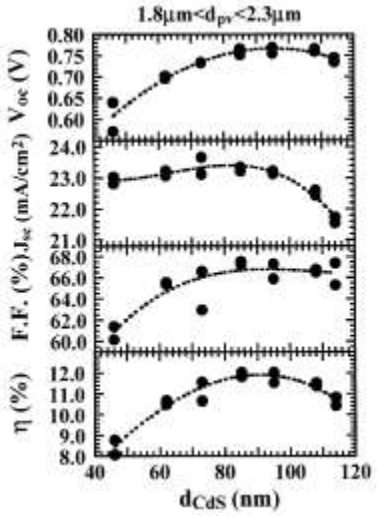

Figure 1.10 J-V performances of CdTe solar cells as a function of CdS layer thickness.
Source: K. Nakamura, M. Gotoh, T. Fujihara, T. Toyama, and H. Okamoto, Sol. Energy Mater. Sol. Cells, 75, 185 (2003).

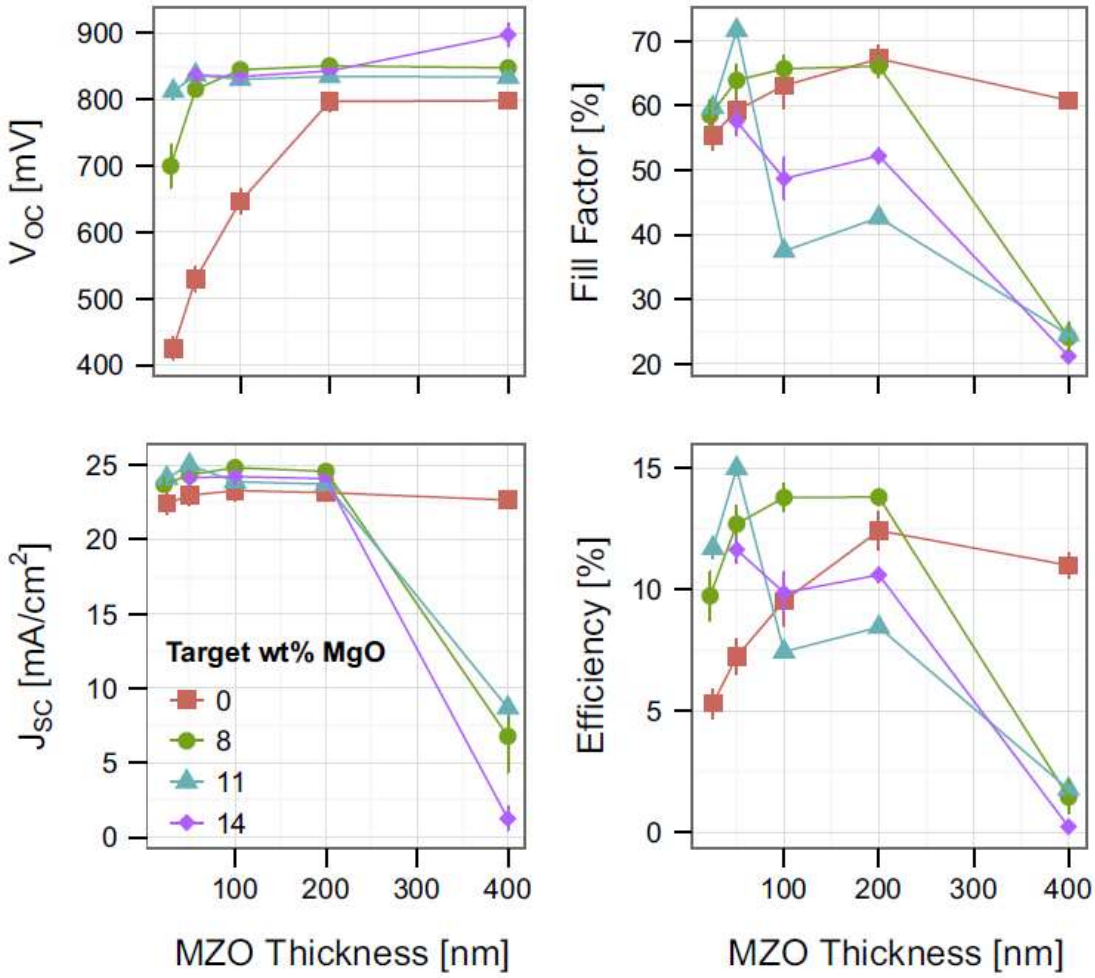

Figure 1.11 Measured J-V results of CdTe solar cells with different Mg content and thickness of ZnMgO layer from CSU.
Source: J. Kephart, J. McCamy, Z. Ma, A. Ganjoo, F. Alamgir, and W. Sampath, Sol. Energy Mater. Sol. Cells, 157, 266 (2016).

The window layer is usually considered to play two roles. First, it should play a role of buffer to prevent the direct contact between TCO layer and CdTe absorber layer. The TCO/CdTe diode is not desired due to the unfavorable band alignment of TCO layer with CdTe, from a combination of electron affinity, charged defects and degenerated doping. That is the reason in early times CdS layer in CdTe solar cells is usually named ‘buffer’. To play a role of buffer, certain thickness is required. But for CdS, big thickness means big

blue loss. To reduce the blue loss, thickness of CdS is reduced and an HRT layer, usually ZnO or SnO_2, is added to plays a role of buffer. CdS, then only play the second role as an electrode to form an n-p junction with p-type CdTe absorber to help separate the photo-generated carriers. For wider band gap materials, ZnMgO as an example, light absorption in the window layer can be ignored and the doping concentration of it can determine what role they are playing. Here, a standard is proposed. If the doping concentration of ZnMgO layer is high, bigger than 10^{17} cm^{-3}, it plays both the role of buffer and electrode. If the doping concentration of ZnMgO layer is low, it only plays a role of buffer. The corresponding structure of CdTe solar cells for each case is also different and will be specifically discussed in Section 5.1. In our previous work [56], the influence of other parameters of ZnMgO layer can change at different doping concentrations, which is a proof that different doping concentration of ZnMgO layer means different structures. Hence, the influence of doping concentration should be seriously investigated.

Although all the four parameters of the window layer has been investigated and discussed by other scientists and researchers, systematic optimization of it still lacks. In this dissertation, we will use wider band gap material ZnMgO to discover the optimal conditions of for the window layer of CdTe solar cells by both simulation and experimental methods. Since we are using ZnMgO as the window layer, the band gap and electron affinity can both be determined by the Mg content. Also, the influence of thickness and doping concentration can be studied together because they together decide the structure of CdTe solar cells.

1.3 TCO Layer of CdTe Solar Cells

The TCO layer is a kind of semiconductor that serves as the front contact for CdTe solar cells. It is also part of the front end. Although it may play less important role on the performance of CdTe solar cells than the window layer, it is still worthy to briefly introduce and optimize this layer.

TCO semiconductor is widely used in solar cells due to its transparence and high conductivity. Without a TCO layer, solar cells cannot work. An ideal TCO material should have the following properties.

(1) The electrical resistivity around 10^{-5} Ω.cm,

(2) High doping concentrations, usually degenerated,

(3) Absorption coefficient smaller than 10^{4} cm^{-1},

(4) Band gap bigger than 3 eV,

(5) Stable in hostile environment containing acidic or alkali solutions, oxidizing and reducing atmospheres, and elevated temperature.

(6) Inexpensive and non-toxic.

Traditionally, Sn doped In_2O_3 (ITO) [57-59] is one of the preferable materials for most present applications. However, due to the high price of Indium, some new TCO materials have been developed to replace ITO, such as F doped In_2O_3 (FTO), Co doped In_2O_3 and Al doped ZnO (AZO). All TCOs are n-type materials, but p-type TCO is also under research and development. So far, no p-type TCO materials are being used in real applications.

The most important characteristics of TCO materials are their optical and electrical properties. In this dissertation, a simple and preliminary model is provided that the

thickness of TCO layer is related to its optical and electrical properties, further the whole performance of CdTe solar modules.

CHAPTER 2

SIMULATION METHOD

SCAPS (a Solar Cell capacitance Simulator) is a one-dimension simulation program which is commonly used for the research of solar cells [60]. The program can build different kinds of solar cell devices by setting up different layers and interfaces between them. It numerically solves Poisson and continuity equations for electrons and holes in one dimension to determine the band diagram of the solar cell devices and their response to illumination, voltage bias and temperature. After that, the performance of the solar cells is simulated by the program, such as J-V, C-V and QE.

In this research, a CdTe solar cell model using ZnMgO as the front end is chosen to do the simulation. We mostly use ZnMgO for two reasons. First, our experimental work is nostly on ZnMgO. Second, leading research groups report that among all the tested window materails, ZnMgO renders the best results. Then the simulated and experimental results can be compared to find out the influence of the window layer on CdTe solar cells. The structure of the CdTe solar cell simulated is shown in Figure 2.1. It is composed of a back contact (Initial setup in the program, flat bands condition, work function of back contact at the same level with the Fermi level of p-type CdTe), a CdTe absorber layer, an interface between CdTe and ZnMgO layer, a ZnMgO window layer, a TCO layer and a front contact (Initial setup, same as back contact). The input parameter of each component is listed in Table 2.1, partly achieved from other publications. [38, 61, 62]

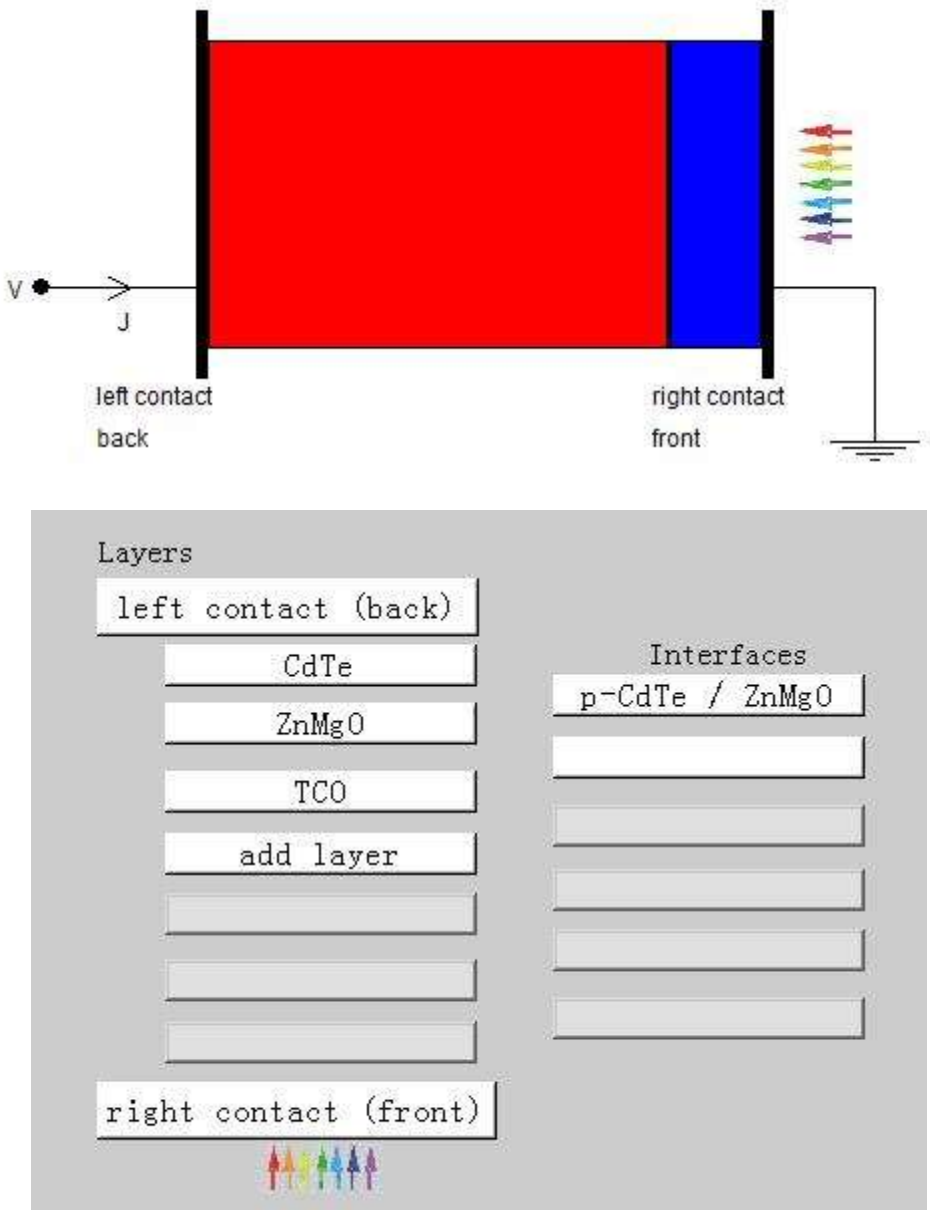

Figure 2.1 The structure of simulated CdTe solar cell.

To simulate the influence of the band gap individually, all the other parameters are kept same while only the value of the band gap of the window layer is changed from ZnMgO's value 3.4eV to CdS's value 2.4eV. Then J-V and QE simulation will be done and the simulated results in the two cases will be compared to make some conclusion.

Table 2.1 Initial Input Parameters of Each Component in the Simulation

Layer	**TCO**	**ZnMgO**	**CdS**	**Interface**	**p-CdTe**
Thickness [nm]	500	70	70	-	2500
Band Gap [eV]	3.7	3.2	2.4	-	1.5
Electron Affinity [eV]	4.5	4.5	4.5	-	4.4
Relative Dielectric Permittivity	10	10	10	-	9.4
Density States of Conduction Band [cm^{-3}]	2.2×10^{18}	2.2×10^{18}	2.2×10^{18}	-	8.0×10^{17}
Density States of Valence Band [cm^{-3}]	1.8×10^{19}	1.8×10^{19}	1.8×10^{19}	-	1.8×10^{19}
Electron Mobility [$cm^2/V.s$]	40	100	100	-	320
Hole Mobility [$cm^2/V.s$]	10	10	25	-	40
Donor Concentration [cm^{-3}]	1.0×10^{19}	1.0×10^{16}	1.0×10^{16}	-	-
Acceptor Concentration [cm^{-3}]	-	-	-	-	1.0×10^{15}
Dopant energy level [eV]	-	0.14	0.14	-	0.255
Deep Level Defect Type	SA*	SA	SA	N*	SD*
Electron Cross Section [cm^2]	1.0×10^{-15}	1.0×10^{-17}	1.0×10^{-17}	1.0×10^{-15}	1.0×10^{-13}
Hole Cross Section [cm^{-2}]	1.0×10^{-12}	1.0×10^{-12}	1.0×10^{-12}	1.0×10^{-15}	1.0×10^{-15}
Defect Concentration [cm^{-2}]	1.0×10^{16}	3.0×10^{15}	3.0×10^{15}	1.0×10^{13}	2.0×10^{13}
Defect energy level [eV]	2.0	1.9	1.12	0.6	0.585

* SA = single acceptor, N = Neutral, SD = single donor

To investigate the influence of electron affinity, we change the value of electron affinity from 3.7 eV to 4.7 eV so that the value of conduction band offset is in the range of -0.3 eV to 0.7 eV. The other input parameters are kept same. Since the electron affinity of ZnO is already 4.3 eV, which means the conduction band offset between ZnMgO and

CdTe is always bigger than 0.1 eV according to Equation (1.2), we have to use CdSO to do the simulation in order to reach a negative value of conduction band offset. All the other input parameters can be kept same; the only difference is the electron affinity. Two different conditions are considered here as to whether or not intra-band tunneling is included. The mechanism of intra-band tunneling is specifically discussed by researchers from University of Gent [64] and will be briefly introduced in Section 4.1 of this dissertation. The simulated J-V results will be plotted. It can be expected that the performance of CdTe solar cells under these two conditions will be quite different.

To investigate the influence of doping concentration and thickness, conditions to specify the structure of CdTe solar cells in terms with the doping concentration and thickness of the window layer is listed first. Various simulations will be subsequently done with same doping concentration but different thicknesses (range from 5 nm to 200 nm) or same thickness but different doping concentrations range from (10^{14} cm^{-3} to 10^{18} cm^{-3}). 3-D plot of the open-circuit voltage, short-circuit current, fill factor, and efficiency of CdTe solar as the function of doping concentration and thickness of the window layer will be provided in order to clearly figure out their influence under different structures of CdTe solar cells. Our recent research indicates that the doping concentration may also influence the intra-band tunneling [53]. Thus, the influence of doping concentration is particularly investigated when the value of conduction band offset is 0.4 eV and intra-band tunneling is included in the simulation.

All the simulated results will be compared with the experimental results to reach the final conclusions. In case there are conflicts between the simulated and experimental

results, deep analysis on the results will be followed to find out what result is more reasonable.

CHAPTER 3

EXPERIMENTAL METHOD

3.1 Processing of the CdTe Solar Cell

In this research, we fabricated CdTe solar cells with a structure of TCO (without HRT)/ ZnMgO/ CdTe/ Cu. However, to find out the influence of the band gap of the window layer, a comparison solar cell with a structure TCO/ CdS/ CdTe/ Cu was also prepared. The specific processing of the CdTe solar cell is listed as following.

3.1.1 TCO

We use commercial FTO glass, Pilkington TEC 12D glass (without an HRT layer), directly as the TCO layer.

3.1.2 ZnMgO

Hollow cathode sputtering system (HCSS) is used to deposit ZnMgO. The parameters of ZnMgO can be controlled as follows.

For the band gap and electron affinity, the sputtering target can be changed with different Mg content so that the band gap of ZnMgO can be altered. Assume common anion rule is right; the electron affinity of the deposited ZnMgO then can be approximately estimated. In our center, we have 15% atomic Mg target, 12% atomic Mg target and 8% atomic Mg target to do the deposition.

For the thickness, it is controlled by the power supplied to the target and the deposition time. The target power is usually fixed at 150W. The thickness is then mainly controlled by the deposition time. The deposition rate for ZnMgO is about 20 nm per minute. The ZMO thickness is not only calculated according to the sputtering power input and and time, it is also directly measured with the instrument.

For the doping concentration, in the hollow cathode sputtering system (HCSS) we have installed a bar that contains some elements as the dopant. In the ZnMgO window layer with no impurity dopants, we assume the oxygen vacancies provide donor defects. In our lab, we also try to use tungsten, aluminum as the dopant. The doping concentration and mobility of ZnMgO can be controlled by the power supplied to the bar. Higher power yields higher doping concentration. The power to the bar is usually set at 5, 10 or 15 W.

3.1.3 CdS

We use chemical bath deposition (CBD) to deposit CdS thin film on the FTO glass. A water bath station, shown in Figure 3.1, was designed and made to set up the deposition.

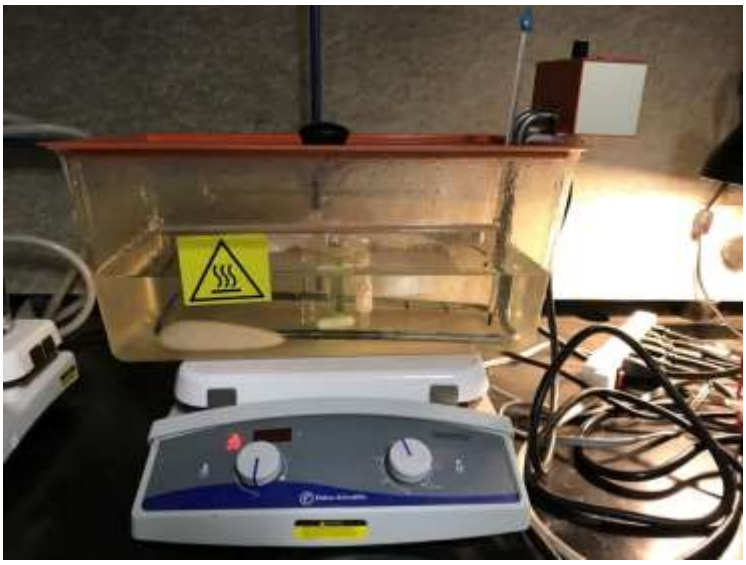

Figure 3.1 The water bath station for CBD.

Four types of chemicals are used, including:

(1) NH_4OH, with a molecular weight of 35.04 g/mol.

It can help maintain the PH of the solution (10.2-11), promote hydrolysis of $SC(NH_2)_2$ to have S ions, also form Cd complex on substrates to prevent homogeneous r*n of Cd^{2+} and S^{2-}. In general, more NH_4OH promotes the heterogonous reaction, but slows down the overall reaction. Homogeneous reaction is favored with decreasing NH_4OH. Concentration of ammonium hydroxide is large with respect to the reactant species.

(2) $CdCl_2$, with a molecular weight of 183 g/mol.

It is used as a source of cadmium ions.

(3) NH_4AC, with a molecular weight of 77.08 g/mole.

It is used as a pH buffer, but excess of NH_4AC reduces the OH^- concentration, which in turn reduces the sulfur ions.

(4) $SC(NH_2)_2$, also named as Thiourea, with a molecular weight of 76.12 g/mol.

Its hydrolysis with OH^- used as a source for sulfur ions, increasing the Thiourea concentration with respect to the cadmium ion concentration drives the hydrolysis of the Thiourea.

The stock solution of the chemical reaction is as following

(1) 100 mL 1M NH_4AC, from 7.708 g powder,

(2) 100 mL 0.1M $CdCl_2$, from 1.8331 g powder,

(3) NH_4OH 15M directly from the bottle,

(4) 100 mL 0.1M $SC(NH_2)_2$, from 0.7612 g powder.

After the stock solution was made, two pieces of 2 cm×2.5 cm substrates is put back-to-back into a beaker with 200mL DI water. Put the beaker into the water bath station, fill the DI water to a level appropriate to the beaker size and increase the temperature by the heater. Then the recipes of the reaction are added into the beaker with the following subsequence when the temperature reaches 80 ºC.

(1) 4mL $CdCl_2$

(2) 8mL NH_4Ac

(3) 8mL NH_4OH, 4*2mL aliquots buffer with 5 minutes interval

(4) 24mL $SC(NH_2)_2$

After all the recipes are added, the deposition rate of the CdS is approximately at 2 nm/min. Wait for another 40 to 60 minutes, then the reaction can be terminated. However, before finishing the reaction, insert a beaker of DI water into the bath for preheating. Once the reaction completes, move the substrates into the beaker with warm DI water for warm rise. This can helps cool down the substrates slowly, which alleviates the film stress and further prevent the sudden peeling of the deposited films.

After the CdS deposition is completed, it needs to be annealed. The annealing procedure can be done in the CSS site before depositing CdTe. The condition for the annealing is 400 ºC, 15 Torr Helium pressure for 15 minutes.

3.1.4 CdTe

In our lab, a small CSS (close space sublimation) equipment is designed and set up to deposit CdTe. The photographs and the description of the chamber are shown in Figure 3.2. Schematic diagram for CSS process is shown in Figure 3.3.

The specific procedure of operating this small CSS will not be discussed here because we find that this equipment is not reliable after multiple time of use. The reason probably is that the thermal couple cannot work well after being used several times so that the real temperature in the chamber is not exactly the number we read from heater. This will influence the sublimation and the result of the deposition may not be perfect as we expect.

Then a big CSS equipment is chosen to deposit CdTe thin films. A source plate of CdTe is first fabricated. The source plate is a prefabricated layer of CdTe film of 2 mm borosilicate glass made using CSS from six-nine CdTe grains. The grains are placed in the 3 mm-deep pocket of the crucible and a piece of 2 mm borosilicate glass was placed at about 4 mm above the surface of the grain using borosilicate glass spacers. The CSS take place at 630/670 ºC with 7 Torr Helium pressure, for 15 minutes. After preparing and inserting the source plate of the crucible into the chamber, the setup is ready to deposit CdTe.

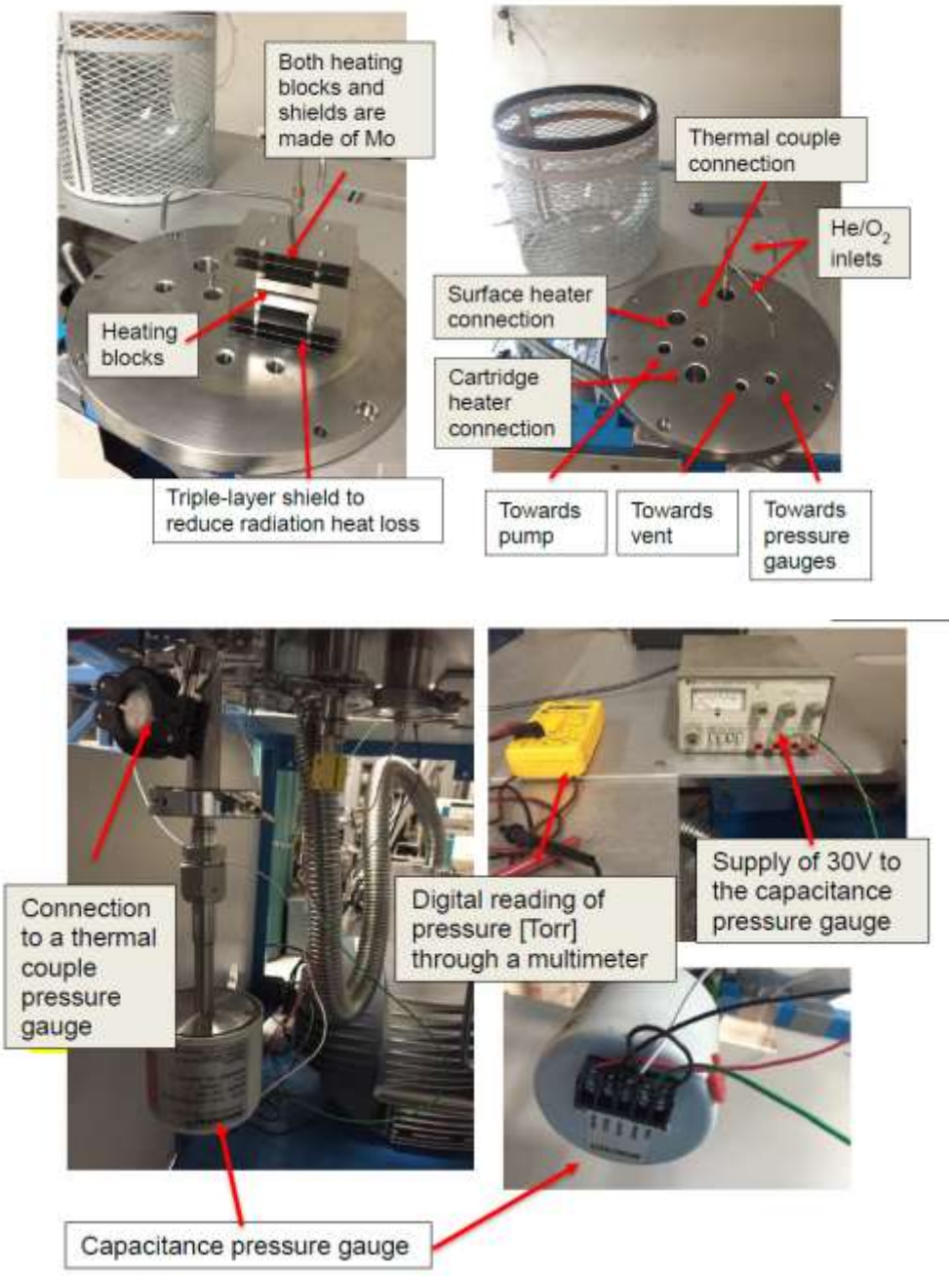

Figure 3.2 The photograph and description of the self-designed small CSS equipment in our lab.

Then we can use the heater to start increasing temperature. The temperature of the superstrate and the source plate during the sublimation are 550 ºC and 630 ºC, respectively

when CdS is used as the window layer. The deposition pressure is 10-15 Torr with Helium. The duration of the deposition is 3 minutes.

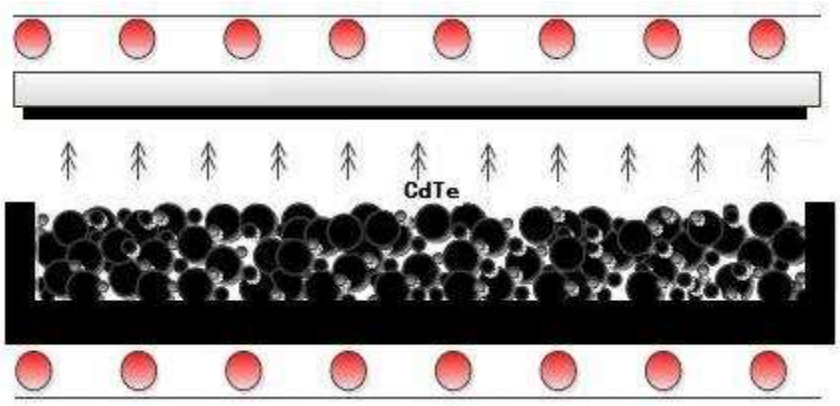

Figure 3.3 Schematic diagram for CSS process.

Here, some notes needs to be reminded during the operation. First, the temperature of the source plate should be at least 50 ºC higher than the superstrate so that the CdTe thin film can be well formed. Second, the temperature difference between the source plate and the superstrate will affect the deposition rate. The larger the temperature difference, the higher the deposition rate. Third, the temperature of the superstrate should be 10 ºC higher than the source plate until reaching the right temperature setting in order to make sure that the there is no actual deposition before that. So, in this research, the temperature setting for the superstrate and the source plate is 480 ºC and 630 ºC, respectively.

CSS has one serious problem. The CdTe powders will frit during the high temperature process, which can prevent them from coming out of the source plate. To avoid this negative effect, we need to increase the temperature of the CdTe crucible or source plate to accelerate the sublimation speed. However, increasing temperature will also

enhance the possibility of fritting since it is an endothermic reaction. Hence, the fritting problem seems insoluble in CSS process and new deposition methods, such as Vapor Transport Deposition (VTD) or Radio Frequency (RF) sputtering, should be considered.

According to many publications from other research groups, $CdCl_2$ treatment is needed to enhance the property of the deposited CdTe thin film. A chamber is used to do the annealing.

Before doing the annealing, we have to measure the thickness of the deposited CdTe thin film. Use blade to cut a line on film for the thickness measurement in order to make sure that the TCO layer will not be hurt. After achieving the thickness of the deposited CdTe thin film, the optimized $CdCl_2$ dose can be calculated through the equation below.

$$y = -2.415 \ln(x) + 8.3409 \quad (3.1)$$

The symbol 'y' here is the coefficient number, which indicates the total solution with 1 ml of saturated $CdCl_2$, whereas the symbol 'x' indicates the thickness of CdTe in the unit of μm. For example, if y calculated is equal to 5, then 1 ml statured $CdCl_2$ solution should be diluted to a total of 6 ml solution with 99.9% alcohol.

After the $CdCl_2$ solution for the annealing is prepared, we then pour the dose carefully on the surface of the CdTe thin film. Wait for approximate 20 minutes until the dose completely evaporates, and a white film on the surface will be seen.

Then, the sample will be put into the chamber facing up. Keep the pressure of the chamber in the range of 200-300 Torr with the flow rate of O_2 and He at 30 sccm and 70 sccm, respectively. Raise the temperature of the chamber to 380 ºC subsequently and last for 40 minutes before stopping the annealing.

3.1.5 Cu

Before depositing Cu, NP etching is needed for the sample after $CdCl_2$ annealing for the purpose of getting a Te-rich surface. The recipe for the NP solution is nitric acid: phosphoric acid: water = 1: 88: 35. The process of NP etching is quite easy, just immerse the sample in NP solution for 15-30 seconds, and rinse it with DI water.

The deposition of Cu in our lab is accomplished in thermal evaporation equipment. After the sample was set in the chamber and the Cu pellet is put in a ceramic coated tungsten basket, open the oil mechanical pump first to lower down the pressure of the chamber to a certain range. Then open the vacuum pump to further pump down into 10^{-4} Torr range. Under these conditions, the layer is not pure Cu layer. Increase the temperature of the chamber by enhancing the current power through the tungsten basket to 60 W. Then the Cu will start to 'brighten', which means it is evaporating. So the duration for this process is 20 seconds. It is not acceptable to increase the current power through the tungsten basket immediately from 0 to 60 W, otherwise the basket may be destroyed. The Cu pellet must be changed after several times of use because it is likely that they may be oxidized.

After the deposition of Cu, carbon electrodag is sprayed onto the sample to make the sample keep off oxygen and moisture. The sample needs to be annealed again in the same equipment doing the $CdCl_2$ annealing at 170 ºC for 20 minutes. This procedure can help on the diffusion of Cu and further form an interface with good properties.

When the annealing on the Cu in is done, 2 mm wide kapton tape was used to cover the back surface and form a grid pattern, where the exposed region was brushed by silver paint. The 2 mm kapton tape grid is removed after drying the silver paint in air for 2

minutes. The grid part where is no silver paint was scribed using a razor blade. The blade is replaced frequently for best scribing performance. The whole back surface of the device is then covered by wide kapton tape and the cell region is masked, exposing the grid region. The substrate is immersed into the PCB board etchant for 10 seconds and rinsed. After drying the sample, indium lines are patterned along the grid by ultrasonic soldering.

Once the back contact is made, the process of fabricating a CdTe solar cell is finished. And the fabricated CdTe solar cell is ready to be measured and characterized now.

3.2 Characterization Methods of ZnMgO and CdTe Solar cell

3.2.1 Characterization of ZnMgO

Once the ZnMgO is deposited, various characterization methods are utilized. We have the FILMETRICS to do the absorption measurement. The transmittance of the thin films can be measured. The absorption coefficient is related to the photon energy from the equation below [63].

$$(\alpha hv)^{\frac{1}{n}} = \beta(hv - E_g) \tag{3.2}$$

here α is the absorption coefficient, hv is the photon energy, E_g is the band gap, β is a constant called the band tailing parameter, *n* is the power factor of the transition mode. We consider ZnMgO a direct band gap material, thus *n* equals 0.5 here. We then can do the tauc plot using $(\alpha hv)^2$ as the y-axis and hv as the x-axis. The plotted gives a straight line in a certain region. The extrapolation of this straight line will intercept the x-axis to give the

value of the optical energy gap. A typical example is shown in Figure 3.4 using CdSO as the n-window.

We also have the Dektak to measure the thickness of ZnMgO thin films. The way to do it is using HCl to make a stage to finish the measurement.

Hall measurement equipment is used to measure the doping concentration and mobility of ZnMgO. The equipment information and the specific process can be found on the website and is skipped here.

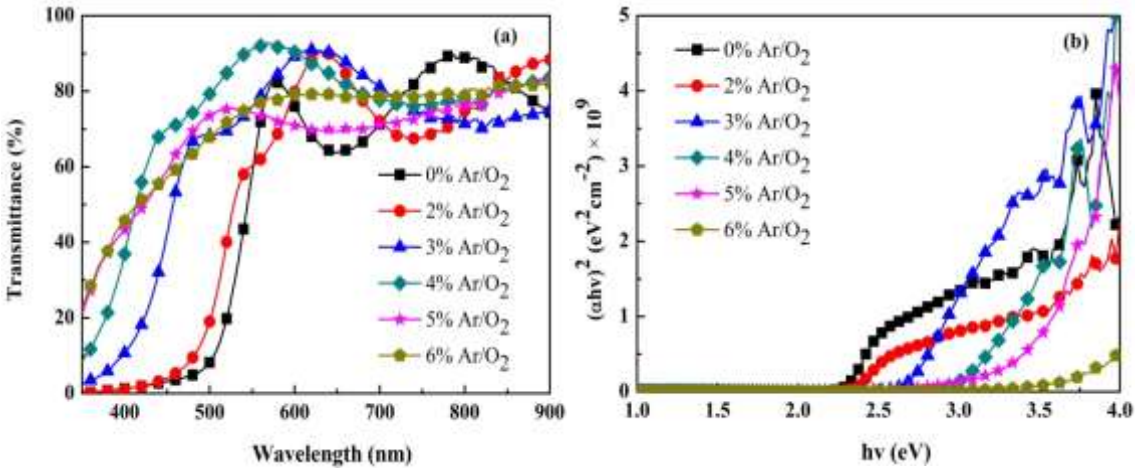

Figure 3.4 The optical properties of the measured CdSO samples.
Note: (a) The transmittance of CdSO samples in terms of wavelength. (b) The Tauc plot of the measured samples.

3.2.2 Characterization of CdTe Solar Cells

A simple stage is set up for the J-V measurement in our lab. A light source is used as the power supply. A program is written in Labview to control the measurement and record the data. The voltage range of the measurement is usually set at -0.6 V to 1.0 V with an interval of 0.02 V. Before doing the J-V measurement, we have to make sure that the light intensity is at 1 sun condition. A CdTe solar cell with an efficiency of 14% was characterized by

University of Delaware. The short-circuit current of the reference solar cell is 17.8 mA. We then put the reference solar cell on the stage and open the light. By adjusting the position of the reference solar cell and the mirror to make the short-circuit current of the reference solar cell to 17.8 mA, we then reach the one sun condition and J-V measurement can be subsequently done. The experimental results will be recorded and plotted.

A simple setup is also made for the QE measurement. A reference solar cell is used to calculate the quantum efficiency and the measured results can be plotted.

CHAPTER 4

THE INFLUENCE OF Mg CONTENT

4.1 Theoretical Analysis

As mentioned in previous sections, the Mg content in the ZnMgO can determine its band gap and electron affinity, further the conduction band offset between CdTe and ZnMgO layer.

Equation 4.1 shows that when the energy of incoming light is bigger than the band gap of a semiconductor layer, it will be absorbed.

$$\frac{hc}{\lambda} \geq E_g \tag{4.1}$$

In this equation, h is the Planck constant, c is the light velocity, λ is the wavelength of light. Since the band gap of CdS is 2.4 eV, light with a wavelength shorter than 520 nm will be absorbed by the CdS, which is not desired as discussed before. The band gap of ZnO is already 3.2 eV, which is big enough to let the incoming visible light go through. With the incorporation of Mg, the band gap of ZnMgO will continue increasing. This means the influence of Mg content on the band gap of ZnMgO is not important for the performance of CdTe solar cells. The primary effect of the increase of Mg content is the increase of conduction band offset.

The influence of Mg content on the conduction band offset can play a significant role on the properties, including open-circuit voltage, short-circuit, fill factor, and efficiency, of CdTe solar cells.

The conduction band offset can influence the open-circuit voltage by influencing surface recombination and built-in voltage of CdTe solar cells. In many heterojunction semiconductor devices, the deep level defects are concentrated at the interface of two layers with different materials. Thus, we assume that most of the electron-hole recombination, which causes the dark current, takes place at the interface in this dissertation. Instead the space charge region Shockley-Read-Hall (SRH) recombination equation, which is widely used, we use the SRH equation for the case of the surface, or interface dark current density and surface recombination rate *(R)* [65-67]. The surface recombination rate then can be expressed as follows [68]:

$$R = \frac{np - n_i^2}{S_p^{-1}(n+n^*)+S_n^{-1}(p+p^*)} \tag{4.2}$$

In the model, p and n is the non-equilibrium concentration for holes and electrons at the interface, respectively. n_i is the intrinsic concentration for the CdTe absorber. S_p and S_n are the surface recombination velocity for holes and electrons at the CdTe / ZMO interface, respectively. The quantity p^* and n^* is defined in Equation (4.3) and Equation (4.4), respectively.

$$p^* = N_V \exp[-(E_D - E_V)/kT] \tag{4.3}$$

$$n^* = N_C \exp[-(E_C - E_D)/kT] \tag{4.4}$$

In these equations, N_V and N_C are the effective density of states in the valence band and conduction band for CdTe absorber, respectively. E_D is the defect energy level at the interface of the CdTe and ZMO . E_V and E_C are the valence band maximum (VBM) and conduction band minimum (CBM) of the CdTe absorber energy level for valence and conduction band, respectively. k is the Boltzmann constant, which is equal to 1.38×10^{-23}

m^2 kg s^{-2} K^{-1}. T is the temperature. The whole term kT is equal to 0.026 eV at normal temperature (300 K).

In this case, at the interface of the window layer and the CdTe layer, n is much larger than p, p^*, and n^*, and np is much larger n_i^2 in non-equilibrium conditions. Assume $S_p = S_n = 10^5\ {}^{\mathrm{cm}}/_{\mathrm{S}}$ here, Equation 4.2 can be simplified as follows:

$$\mathrm{R} = S_p p \tag{4.5}$$

The concentration of holes from the CdTe absorber side at the interface dominates the surface recombination rate. So, p can be expressed as follows:

$$p = N_V \exp(-E_p/kT) \tag{4.6}$$

Here, E_p is called the "hole barrier" and can be expressed as follows:

$$E_p = BB + \Delta E_p \tag{4.7}$$

BB is the band bending, and ΔE_p is defined as the distance between the quasi Fermi level for holes (E_{Fp}) and the valence band maximum energy level of the CdTe absorber layer. Below is the expression for ΔE_p deduced from Maxwell-Boltzmann's distribution equation.

$$\Delta E_p \cong -\mathrm{kT} ln(\frac{N_A}{N_V}) \tag{4.8}$$

In this equation, N_A is the doping concentration of the CdTe absorber, and is a constant for 10^{15} cm^{-3}. Thus, E_p is mainly dominated by band bending. It can be expected that the band bending will increase with the conduction band offset due to the raising of the Fermi-level of the window layer. Thus, together with p, the surface recombination rate will also decrease with the increase of ΔE_C. With a smaller surface recombination rate, the lifetime for electrons (τ_n) will increase.

The saturation current density then will decrease from Equation (4.9) due to the increase of the lifetime for electrons.

$$J_0 \propto \frac{qn_iW}{\tau_n} \tag{4.9}$$

Here, q is the charge of an electron, which equals $1.6*10^{-19}$ C. W is the width of the depletion region, which is mainly determined by the doping concentration of the layers that form the diode, and is independent of ΔE_C. Thus, the saturation current density is reverse proportional with the conduction band offset. Since V_{OC} is related to J_0 as Equation (4.10) indicates.

$$V_{OC} = \frac{AKT}{q}\ln(\frac{J_{SC}}{J_0}) \tag{4.10}$$

A is the diode quality factor. From this relationship, open-circuit voltage is inversely proportional with the saturation current density, and should be proportional with the conduction band offset. Thus, with a smaller electron affinity of the window layer and a bigger conduction band offset, the open-circuit voltage of CdTe solar cells can be enhanced. This means that if we use ZnMgO as the window layer, the open-circuit voltage of CdTe solar cells can be improved by increasing the Mg content. The precondition is the common anion rule is right.

However, V_{OC} cannot increase indefinitely, as it has an upper limit. In this work, an empirical equation is proposed, which establishes a relationship between the upper limit of V_{OC} and built-in voltage (V_{bi}).

$$V_{OC} < V_{bi} = {}^{1}/_{q}\,(E_{gp} + \Delta E_C - \Delta E_n - \Delta E_p) \tag{4.11}$$

The flat band diagram of a typical CdTe solar cell with CdS as the front end is shown in Figure 4.1(a). All the symbols and their approximate value in Equation **(**4.11) are

listed in the figure. For the traditional CdTe solar cells, the upper limit of open-circuit voltage is 1.0 V, but it can still be increased with ΔE_C when wider band gap window is used. However, this equation cannot be always right when ΔE_C becomes positive, the case of 'spike', and continues increasing. The reason is that the quasi-Fermi level splitting is impossible to be more than the CdTe absorber band gap, and the Fermi level of window layer, here CdSO as an example, will be effectively pinned at or below the CdTe absorber conduction band when ΔE_C is the 'spike' case, as shown in Figure 4.1(b). Then V_{OC}, as well as V_{bi}, can only increase slightly, but no longer linearly with the conduction band offset.

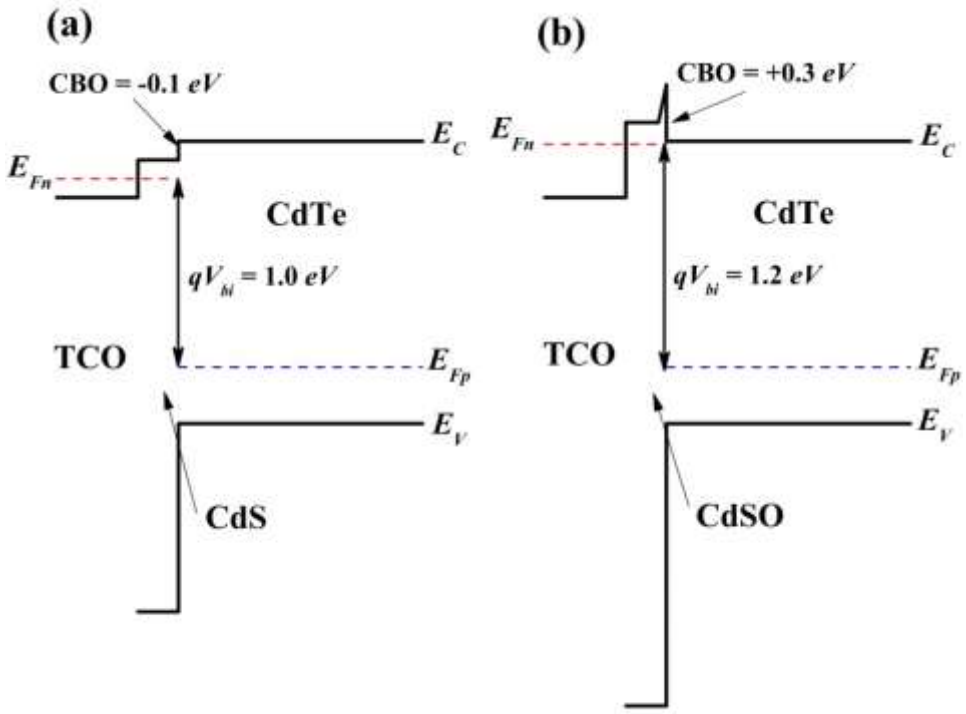

Figure 4.1 Flat band diagrams of CdTe solar cells.
Note: (a) Traditional CdTe solar cell structure with CdS as the window layer. (b) Optimized CdTe solar cell structure with CdSO as the window layer.

Although a higher conduction band offset is beneficial for the open-circuit voltage of CdTe solar cells, a too big conduction band offset is harmful to the short-circuit current. The reason is when the value of conduction band offset is positive; the 'spike' acts as a barrier for the movement of photo-generated electrons. The electrons then need the thermal energy to climb through the 'spike'. This mechanism is defined as thermionic emission and the thermionic emission current density (J_{TE}) can be approximately calculated by the following equation.

$$J_{TE} = A^* T^2 \exp(-q\phi_B/kT) \tag{4.12}$$

A^* here is the Richardson constant, which equals to,

$$A^* = \frac{4\pi m^* k^2}{h^3} \tag{4.13}$$

m^* is the effective mass of an electron in the CdTe absorber, which is equal to $0.11m_0$, or $1.0*10^{-32}$ kg. h is the Planck constant, which equals $6.63*10^{-34}$ J.s.

ϕ_B in Equation 6.11 is the barrier height for electrons, and is the distance between the maximum point of E_C at the interface, and the quasi Fermi level for electrons (E_{Fn}) of CdTe absorber. In this case, we can regard ΔE_C as ϕ_B since the difference between them is negligible. Putting the value of all the parameters into Equation (4.12) and Equation (4.13) above, we can find the calculated J_{TE} will be extremely small when ΔE_C is larger than 0.5 eV. The calculated thermionic emission current density as a function of conduction band offset is plotted in Figure 4.2.

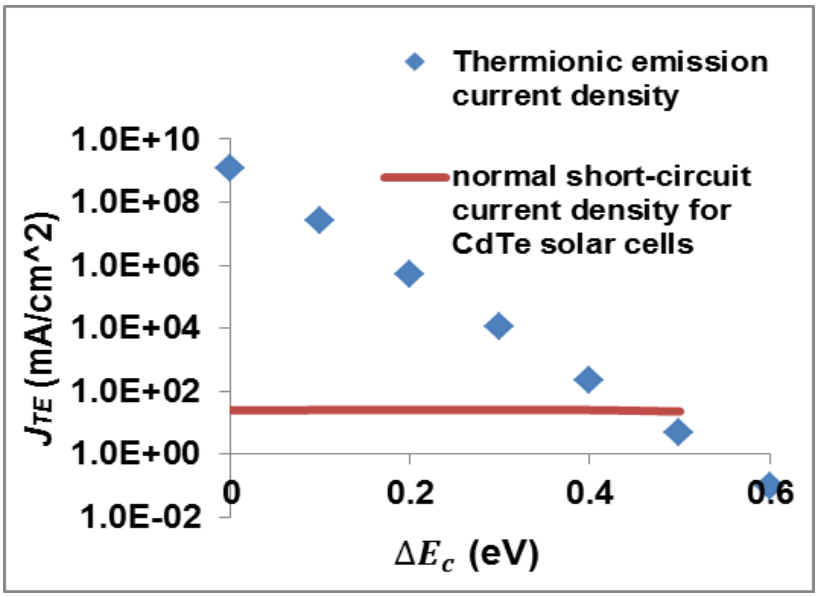

Figure 4.2 The calculated thermionic emission current density.

So, it can be expected if the conduction band offset is too big, the solar cell will fail to work. This means the increasing of Mg content in ZnMgO may not good for the short-circuit current. However, another mechanism should be considered, which is named the intra-band tunneling. Intra-band tunneling allows the electrons tunnel through the 'spike'. Thus, with the intra-band tunneling included, the conduction band offset should be higher before CdTe solar cells fail to work.

The schematic diagram of intra-band tunneling is shown in Figure 4.3. It is a model from other researches' work [62]. They mentioned intra-band tunneling is a combination of thermionic emission and field emission. Detailed derivation is omitted here, but with the intra-band tunneling included, the final net electron current density crossing (J_{net}) the interface in their model is calculated as follows.

$$J_{net} = -\frac{A^*T}{k}\int_{E_C^{min}}^{\infty} f\left(E_x - E_{Fn}^{left}\right)T(E_x)dE_x + \frac{A^*T}{k}\int_{E_C^{min}}^{\infty} f\left(E_x - E_{Fn}^{right}\right)T(E_x)dE_x \quad (4.14)$$

$E_x - E_{Fn}$ is the occupation probability, $T(E_x)$ is the tunneling probability derived from the WKB approximation for free electron mass. It is equal to unity for energies above E_{Cmax}. The lower limit E_{Cmin} is the minimum energy level for which free electron states exist at both sides of the spike. Assume the depletion region in the front end is 10 nm, the calculated net current density crossing the interface is shown in Figure 4.4. From the calculated result, taking the intra-band tunneling into consideration, the net current density crossing the interface will not reduce to a low level even when the conduction band offset is 0.8 eV. Thus, the negative influence of a relatively big conduction band offset on the short-circuit current can be neglected.

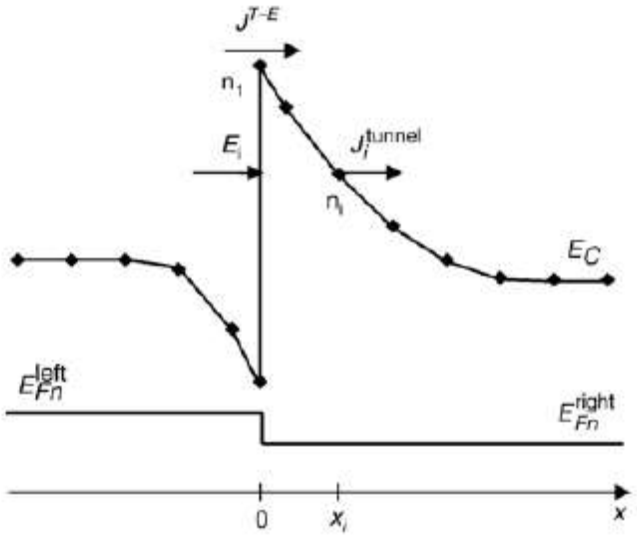

Figure 4.3 Schematic diagram of the intra-band tunneling mechanism.
Source: J. Verschraegen, M. Burgelman, (2007), Numerical modeling of intra-band tunneling for heterojunction solar cells in SCAPS, Thin Solid Films, 515, 6276.

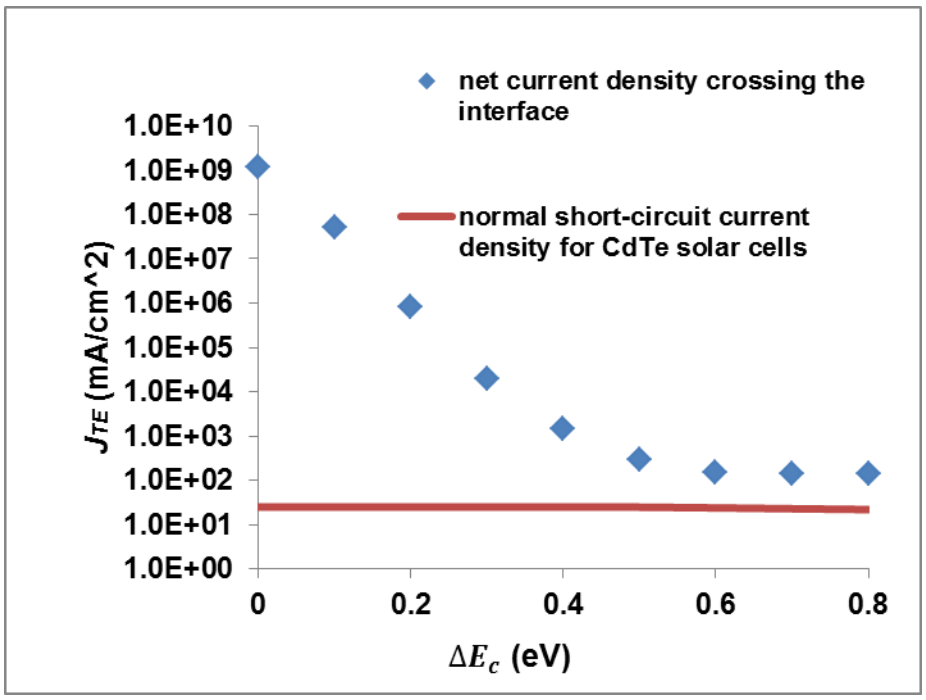

Figure 4.4 The calculated net current density crossing the interface as a function of conduction band offset.

Fill factor of a solar cell is mainly influenced by the series resistance, the shunt resistance, the recombination rate, and the saturation current density of the junction [69]. If the recombination rate is high and the carrier lifetime is relatively low, the recombination in the space charge region may overweight the recombination in the regions outside the space charge region, reducing the ideality factor of the diode and consequently reducing the squareness of the J-V characteristics and the fill factor. Since we have argued that the surface recombination rate can be reduced with the increase of conduction band offset, it can be expected that the fill factor will also be enhanced with the conduction band offset. However, if the conduction band offset is too big, the 'spike' can act as a secondary barrier, leading to a kink in the J-V curve and the decrease of the fill factor. If the intra-band

tunneling is taken into consideration, the electrons can tunnel through the 'spike' and it is not regarded as a barrier anymore.

The efficiency of a solar cell is a combined result from its open-circuit voltage, short-circuit current, and fill factor, as Equation 4.15 indicates.

$$\eta = V_{OC}.J_{SC}.FF \tag{4.15}$$

It can be estimated that the efficiency will go up when the conduction band offset is increased from a negative value to a slightly positive value, but will go down when the conduction band offset continues increasing. So, an optimized value or range for the conduction band can be found and the Mg content in ZnMgO layer can be determined.

4.2 Simulated Results

Firstly, two different CdTe solar cells are simulated with ZnMgO and CdS as the window layer, respectively in order to find out the influence of the band gap. The simulated results are shown in Figure 4.5. Here, we have to mention that the only change of the input parameter is the band gap of the two materials. In reality, when the ZnMgO is used as the window layer, the conduction band offset is impossible to be a negative value like CdS. But to investigate influence of the band gap individually, we keep the electron affinity of the two window materials same at 4.5 eV, so the corresponding value of the conduction band offset is -0.1 eV.

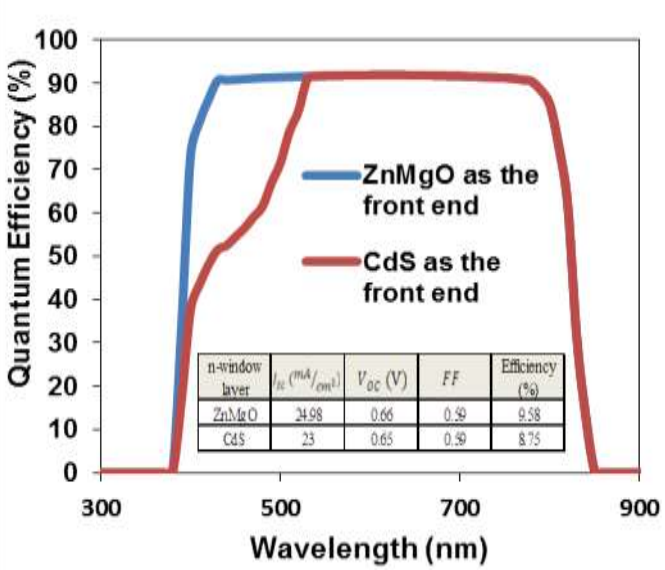

Figure 4.5 Simulated results of CdTe solar cells with different materials as the window layer.

From the simulated results, the removal of blue loss is obvious when wider band material is applied, which contributes an increase of short circuit current by 2 mA/cm^2. However, the open-circuit voltage and fill factor of the simulated CdTe solar cells do not show any tendency of increase. This result does not meet the experimental data from the Colorado State University [47]. The reason is that we keep the electron affinity of the two materials exactly same. Actually, the purpose of introducing a wider band gap material as the window layer is not only removing the band gap, but also adjusting the conduction band offset between the window and CdTe layer.

Then simulation must be done to investigate the influence of the conduction band offset by changing the electron affinity of the window layer. The simulated results are shown in Figure 4.6. As mentioned in Chapter 2, two conditions with whether or not intra-band tunneling is included are considered.

The influence of conduction band offset on the open-circuit voltage of CdTe solar cells is quite same under both conditions. The simulated results show that the open-circuit voltage of CdTe solar cells increase almost linearly with the conduction band offset at first, which meets the theoretical analysis. To further prove this improvement of the open-circuit voltage is originated from the decrease of surface recombination, the simulated Fermi distribution at the open-circuit condition and the recombination rate at the surface area at three different values of conduction band offset are plotted in Figure 4.7 and Figure 4.8, respectively. From Figure 4.7, we can find that the band bending increases with conduction band offset due to the raising of the Fermi-level of the window layer. Thus, according to the equations mentioned above, the surface recombination should decrease against the increase of conduction band offset, which is certified in Figure 4.8. Here the defect concentration at the interface is set at 10^{13} cm^{-2}. Additional drawings on the open-circuit voltage of CdTe solar cells as a function of the conduction band offset at other different defect concentration at the interface is plotted in Figure 4.9. From the figure, it is obvious that the influence of the conduction band offset on the open-circuit voltage is negligible when there is no interface defect. However, the influence of the conduction band offset becomes more severe with the increase of the interface defect density. The interface defect density cannot be higher than 10^{15} cm^{-2} due to limitation of atomic density, usually in the magnitude of 10^{21} cm^{-3} to 10^{23} cm^{-3}. This is another proof that a positive conduction band offset, the case of 'spike', can help reduce the surface recombination.

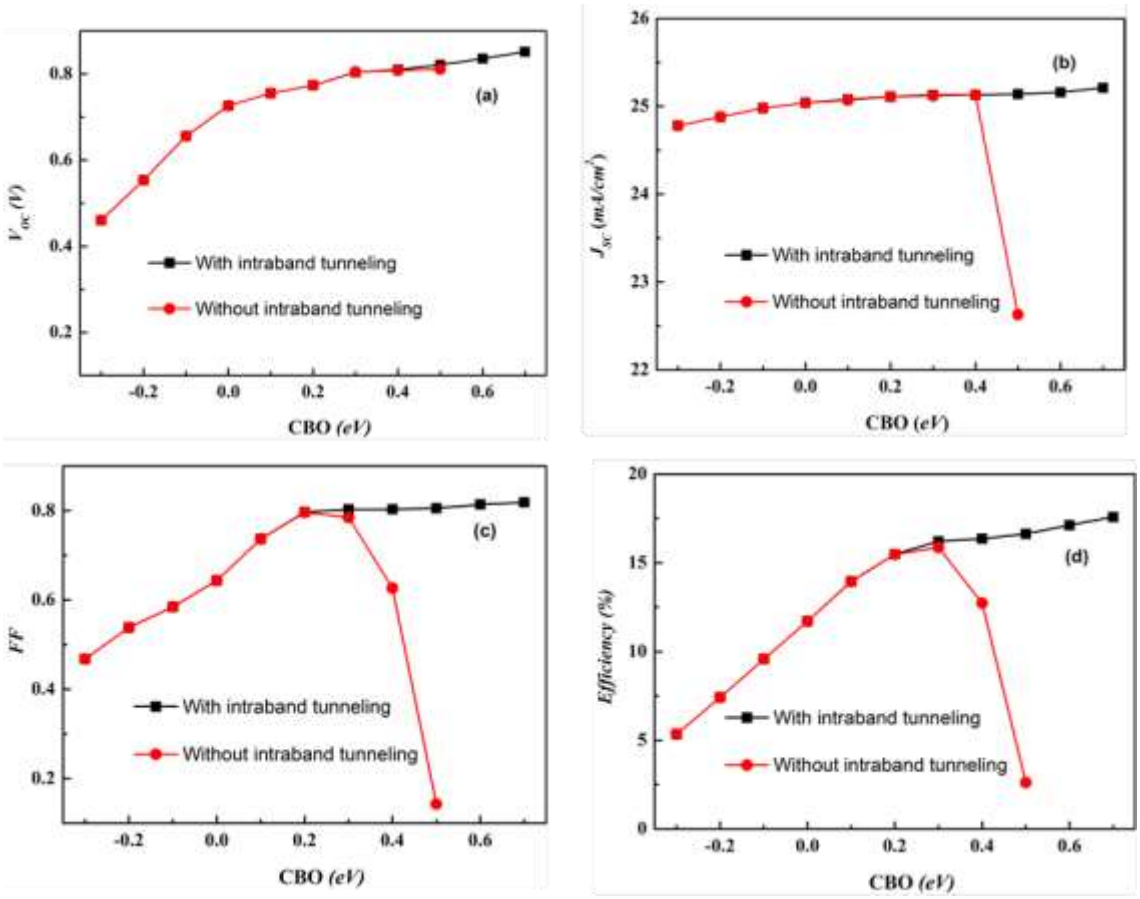

Figure 4.6 Simulated performance of CdTe solar cell as a function of ΔE_C.
Note: (a) V_{OC} as a function of ΔE_C. (b) J_{SC} as a function of ΔE_C. (c) FF as a function of ΔE_C. (d) Efficiency as a function of ΔE_C.

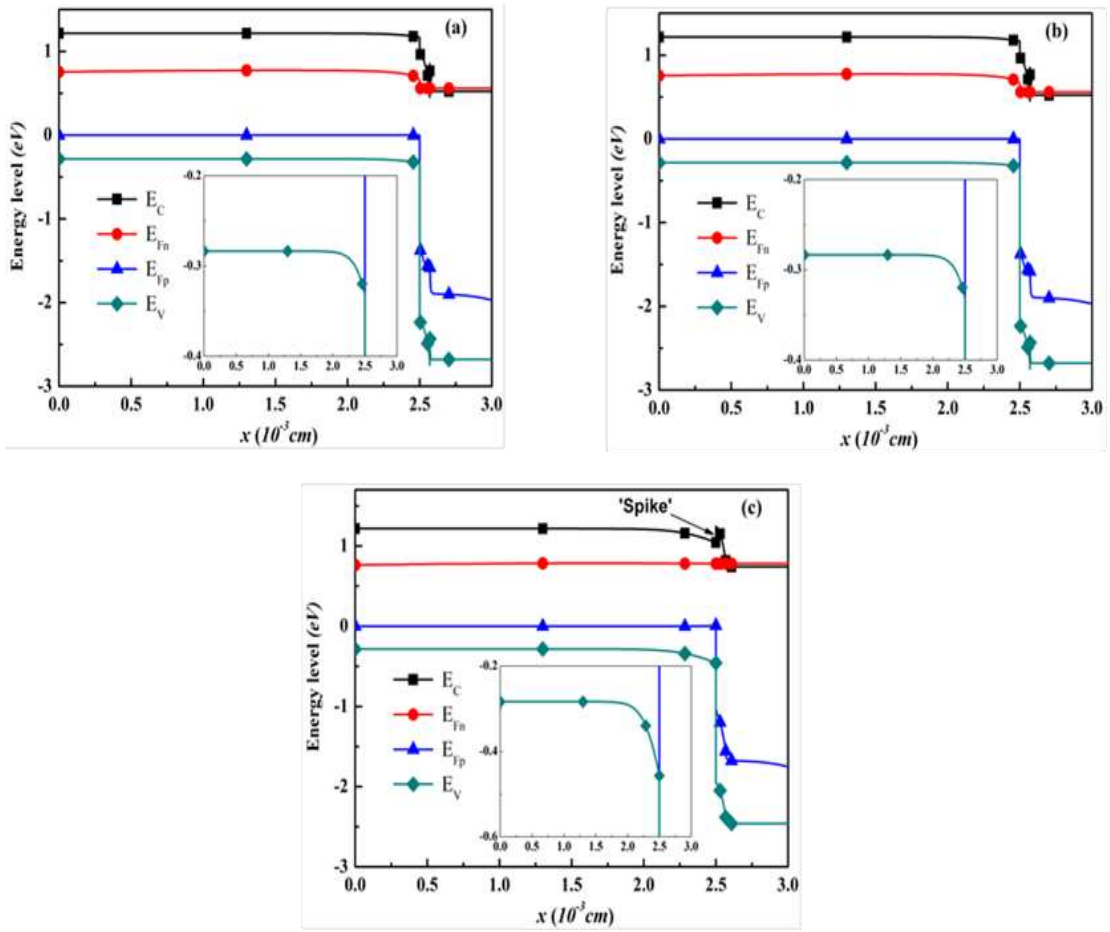

Figure 4.7 Simulated band diagram of CdTe solar cells at different ΔE_C with band bending enlarged at open-circuit condition.

Note: (a) ΔE_C=-0.2 eV. (b) ΔE_C=0 eV. (c) ΔE_C=0.2 eV. x is the vertical spatial dimension of the simulated CdTe solar cells.

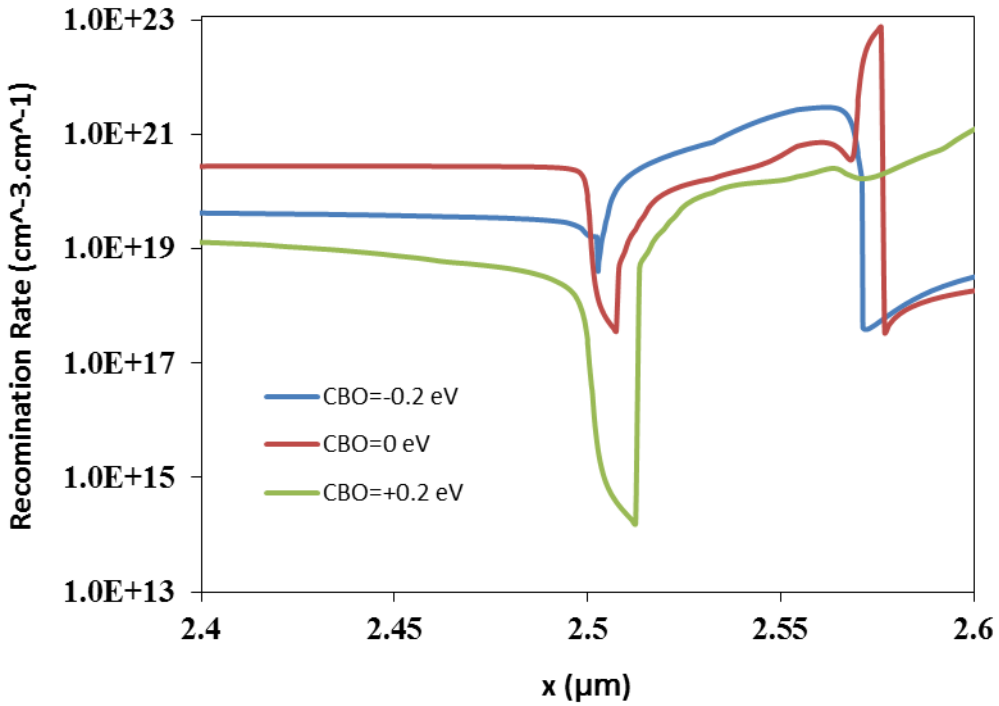

Figure 4.8 Simulated recombination rate near the interface areas.

Simulated results also show that the open-circuit voltage only increases slightly with the conduction band offset, which is again within the expectation. This is because of the limitation of the built-in voltage, which in this simulation case should not be higher than 1.1 V. Meanwhile, some other issues may also limit the open-circuit voltage. That is why our simulated open-circuit voltage is not higher than 0.95 V.

The influence of conduction band offset on the short-circuit current should be separately considered under the two different conditions. Under both cases, short-circuit current of CdTe solar cells remains almost a constant before conduction band offset reaches 0.4 eV. This is due to the band gap of CdTe absorber itself. However, if the intra-band tunneling is not included, the short-circuit current of CdTe solar cells reduces dramatically when the conduction band offset reaches +0.5 eV. The simulation even

suffers convergence failure when the conduction band offset continues increasing. This perfectly matches our theoretical model. On the other hand, if the intra-band tunneling is included. There is no decrease of the short-circuit current against the increase of conduction band offset, which is also within our theoretical model.

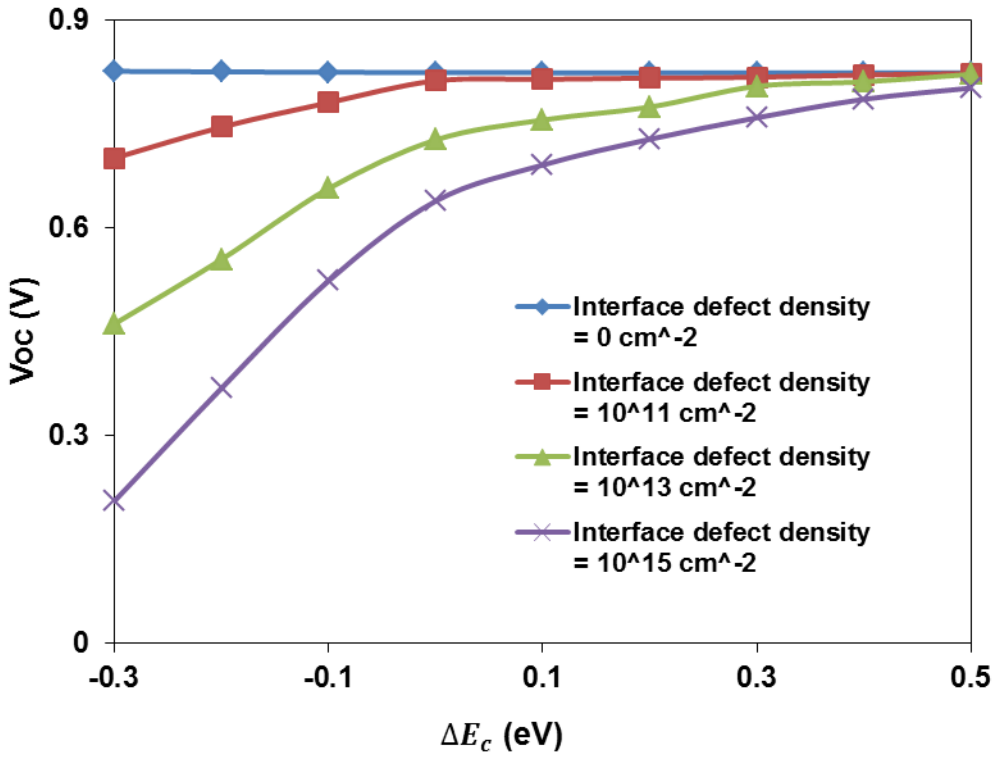

Figure 4.9 Open-circuit voltage as a function of conduction band offset at different interface defect density.

Simulated results show that the fill factor increases dramatically with the conduction offset at first, resulting from the decrease of surface recombination rate, as expected. The fill factor drops down later in the case that intra-band tunneling is not included in the simulation, which means a big value of conduction band offset can act as a

secondary barrier for the photo-generated electrons. The fill factor does not drop down in the case that intra-band tunneling is included in the simulation, which means this mechanism can help electrons tunnel through the 'spike', and a big value of conduction band offset is not considered as a secondary barrier anymore.

The influence of conduction band offset on the efficiency of CdTe solar cells is a combination of its influence on the open-circuit voltage, short-circuit current and fill factor. If intra-band tunneling is not included, there is a balance between the increase of open-circuit voltage and decrease of short-circuit current and fill factor with the increasing value of conduction band offset and the optimized efficiency of CdTe solar cells stays in the range of 0.2 eV to 0.3 eV. However, if intra-band tunneling is included in the simulation, a bigger conduction band offset seems to yield a higher efficiency of CdTe solar cells.

Although our theoretical model proposed in this dissertation perfectly matches the simulated results, there is possibility that it does not exactly meet the real experimental data; especially the intra-band tunneling may not happen under certain circumstances. Considering other researchers' model and results [38, 50], to be safe, the conduction band offset recommended from the simulated data is 0.3 eV. It is a value that using ZnMgO as the window can achieve, and the corresponding band gap and electron affinity for ZnMgO is 3.5 eV and 4.1 eV, respectively. Putting the value of this band gap into Equation (1.1), the optimized atomic Mg percent in ZnMgO should be around 10%.

.

4.3 Experimental Results

CdTe solar cells are fabricated using ZnMgO, by Radio Frequency (RF) Sputtering and HCS, and CdS as the window layer, respectively to investigate the influence of band gap of the window layer. The measured QE results are shown in Figure 4.10 [70]. The removal of blue loss is again experimentally proved. Short-circuit current is increased from 20.4 mA/cm^2 (dash black line using CdS as the window layer) to 25.9 mA/cm^2 (solid blue line using HCS ZnMgO as the window layer). The figure also shows the superiority of HCS on the deposition of ZnMgO to achieve of higher quantum efficiency. This proves the advantage for the adoption of wider band gap materials as the window layer.

The J-V curves measured in dark and under solar illumination of the CdTe solar cell, solid blue line in Figure 4.10, are plotted in Figure 4.11. The open-circuit voltage, 0.836 V, and short-circuit current, 25.9 mA/cm^2, of the solar cell is pretty good, just a little smaller than that of Colorado State University [45]. However, our cell's extreme poor fill factor, 0.431, leads to the low efficiency at only 9.3%. The undesired shape of the J-V curve under light condition indicates that the electron collection efficiency deteriorates as the output voltage increases [71]. The electron collection efficiency is related to the back contact and its role as the electron reflector [72], as well as many other factors, which are beyond the scope of this dissertation. The big sheet resistance probably comes from a too big conduction band offset, which can also lower down the fill factor. For this sample, the atomic Mg percent in the ZnMgO layer is 15%. This is the value achieved from a publication from the research group in Colorado State University [47]. The corresponding conduction band offset is 0.42 eV, which is bigger than our proposed optimal range. The measured value of fill factor meets the simulated results under conditions that the intra-band tunneling is not included.

This means in this CdTe solar cell, intra-band tunneling is not happening. All the measured experimental results and the analysis on it lead to a conclusion that the Mg content in ZnMgO must be precisely controlled. For our center, the Mg content should be reduced in ZnMgO layer. Thus, a new target with 12% atomic Mg content is now under using. The corresponding conduction band offset then becomes 0.35 eV, which should bring a much better performed CdTe solar cell based on the simulated results.

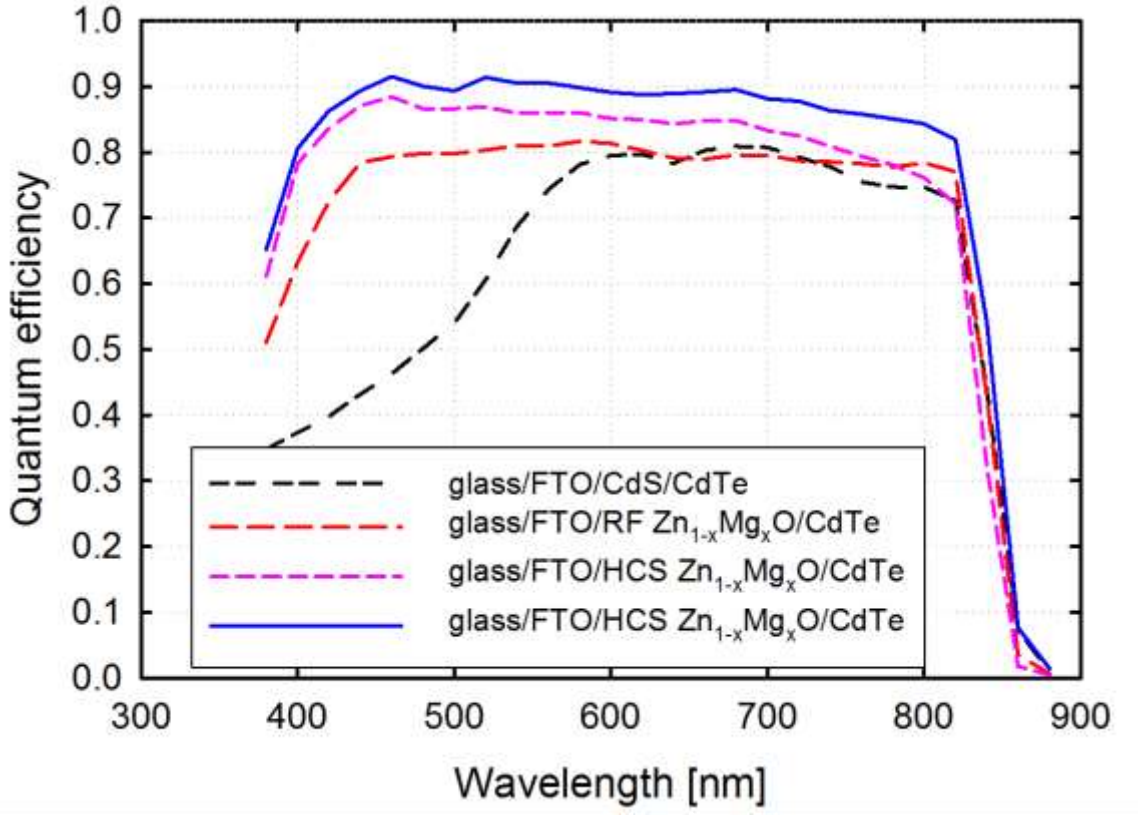

Figure 4.10 QE measurement results of the fabricated CdTe solar cells using different kinds of window layer materials.
Source: A. Delahoy, S. Peng, P. Patra, S. Manda, A. Saraf, Y. Chen, X. Tan, and K. Chin, in Proceedings of MRS Advances (2017), pp 1-12.

Two CdTe solar cells have been processed using ZnMgO with 12% atomic Mg content and ZnMgO with 15% atomic Mg content as the window layer, respectively. The other conditions during the deposition of ZnMgO are exactly same, only the target is changed. J-V characterization has been done for the purpose of finding out the influence of the Mg content.

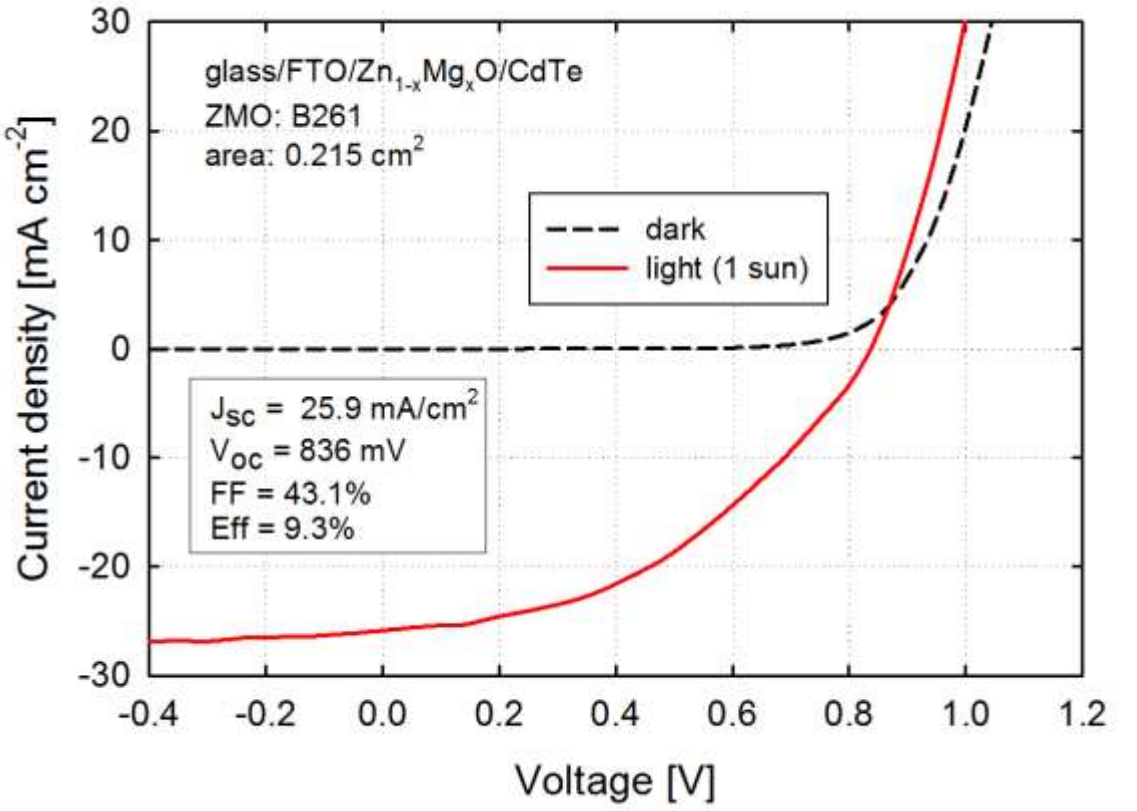

Figure 4.11 J-V measurement results of the fabricated CdTe solar cell using HCS ZnMgO as the window layer.

The measured J-V results for the two CdTe solar cells are shown in Figure 4.12. From the experimental results, we can find the CdTe solar cell made by 12% atomic Mg content ZnMgO is better than that made by that made by 15% atomic Mg content ZnMgO

with a much higher short-circuit current and fill factor, but lower open-circuit voltage. The appearance of a kink in the blue line proves that a big conduction band offset can act as a secondary barrier for the photo-generated electrons. The kink disappears in the green line when 12% atomic Mg content ZnMgO is used as window layer and the fill factor becomes much better. However, the green line solar cell's fill factor is still quite small at only 0.51. One possible reason is that 12% atomic Mg content is still too big since the simulated results reveals 10% is the best. Another possible reason is that the mobility×lifetime product is low for minority carriers in the CdTe absorber layer. Finally, the process for the back contact of our center's CdTe solar cell is not perfect.

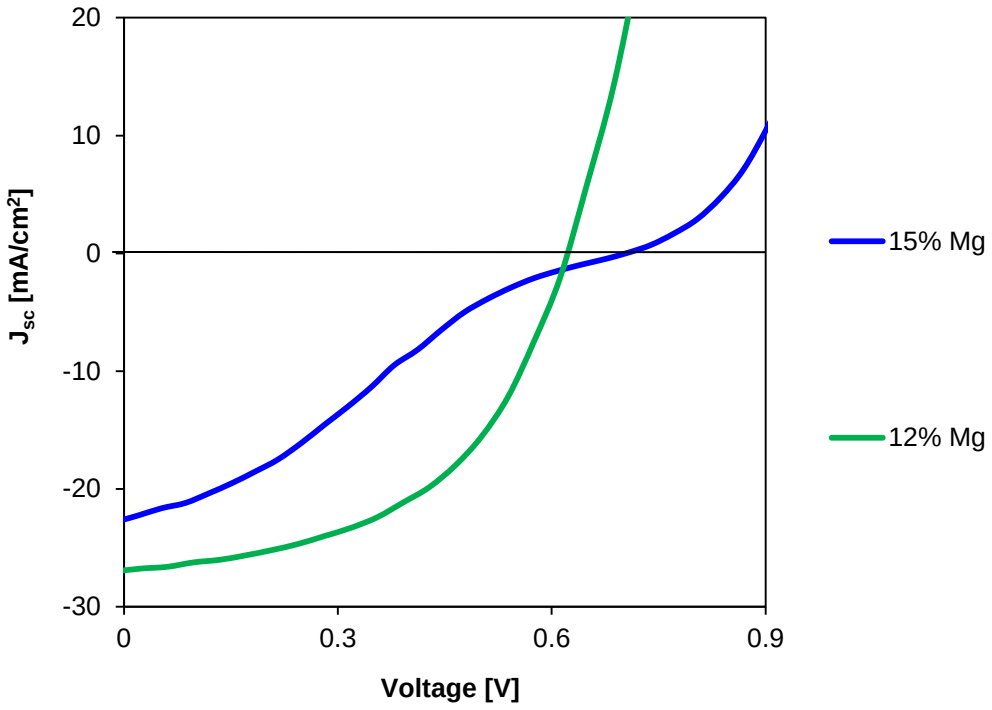

Figure 4.12 J-V results of CdTe solar cells using ZnMgO with 15% atomic Mg content and 12% atomic Mg content, respectively, as the window layer.

Both the simulated and experimental results indicate that precise control of the atomic Mg content in ZnMgO is very important, not to change its band gap but to adjust the conduction band offset. Simulated results show 10% atomic Mg content, resulting in a 0.3 eV conduction band offset, is suitable to achieve best performance of CdTe solar cells. Experimental results shows a better performance of CdTe solar cells when the atomic Mg content is reduced from 15% to 12%. While FTO/ZnMgO substrates have been deposited with 8% atomic Mg, more CdTe solar cells using ZnMgO with smaller atomic Mg content, such as 10% or 8%, as the window layer should have been processed in order to more accurately find out the optimal value or range on the atomic Mg content of ZnMgO layer. It has not been done so far due to the limited resources of our center. But the tendency resulted from the decrease of the atomic Mg content can help us make a prediction that using ZnMgO with a 10% atomic Mg content should yield a better performance on CdTe solar cells. Thus, a 10% atomic Mg content is strongly recommended.

CHAPTER 5

THE INFLUENCE OF THICKNESS AND DOPING CONCENTRATION

5.1 Theoretical Analysis

Even wider band gap ZnMgO was used in this dissertation to investigate the influence of thickness for the window layer; there is still reflection of the incoming light in this layer, which can decrease the quantum efficiency and short-circuit current of CdTe solar cells. However, this kind of loss may be negligible. But the thickness of the window layer is still possible to affect the properties of CdTe solar cells from other aspects.

As discussed in previous chapters, the window layer of CdTe solar cells can play two roles. It must act as buffer to prevent the unfavorable direct contact between the CdTe absorber layer and the TCO layer. It can also serve an electrode to form an n-p junction with CdTe absorber. Whether or not the window layer plays a role of electrode is mainly determined by its doping concentration. The doping concentration together with the thickness of the window layer can determine the structure of CdTe solar cells. Since the thickness of the window layer usually only varies from 10 nm to 100 nm, the structure of CdTe solar cells is mainly determined by the doping concentration. The name and conditions for each structure is listed in Table 5.1. Charge neutrality in the depletion region must be maintained in the space charge region, as Equation (5.1) shows.

$$\mathrm{n}x_n = px_p \tag{5.1}$$

n, *p* is the doping concentration of window layer and CdTe absorber layer, respectively. x_n and x_p is the depletion width in the window layer and CdTe absorber layer, respectively.

The depletion width in the CdTe absorber layer is usually about 1 μm [73, 74]. When the doping concentration of the window layer is higher than 10^{17} cm^{-3}, then the depletion width in the window layer will be smaller than 10 nm. Usually, the thickness of the window layer is bigger than 10 nm and an n^+-p junction can be successfully formed between the window and CdTe. Electrons from TCO do not have to come to maintain the charge neutrality. However, when the doping concentration of the window layer is reduced, then the depletion width in the window layer becomes bigger. Since the thickness of the window layer usually cannot be higher than 100 nm, an n-p junction cannot be formed just between the window layer and the CdTe absorber layer when the doping concentration of the window layer is smaller than 10^{16} cm^{-3} according to Equation (5.1). Then the depletion region reaches the TCO layer to retain charge neutrality. This kind of structure we call it n^+ (TCO)-n (window)-p (CdTe) structure. When the doping concentration of the window layer is too small, smaller than 10^{15} cm^{-3}, the window layer can be treated as an insulator or resistor layer and almost has no contribution to the charge neutrality and can be treated as an insulator layer, the structure of CdTe solar cells then becomes metal (TCO)-resistor (window)-semiconductor (CdTe), in abbreviation MRS. The n^+-n-p structure can be regarded as a mixture of n^+-p and MRS structure.

Table 5.1 Conditions to Determine the Structure of CdTe Solar Cells

Structure of CdTe solar cells	**Doping concentration of the window layer** cm^{-3}
n^+-p junction	$\geq 10^{17}$
n^+-n-p	10^{15} to 10^{17}
MRS	$\leq 10^{15}$

Therefore, it is valuable to investigate the influence of thickness of the window layer under various doping concentrations.

In case of an n^+-p junction, the thickness of ZnMgO is expected to have negligible influence on the performance of CdTe solar cells if the diffusion length of the electrons is bigger than the ZnMgO's thickness. However, since ZnMgO layer plays a role of buffer, certain thickness is needed to grantee the uniformity of the thin film. In case of an MRS structure, the increasing thickness of ZnMgO can compel the electrons to tunnel through this insulator layer. The electrons must go through the conduction band of the ZnMgO layer, which can be considered as a resistance. The resistivity (ρ) of the ZnMgO is influenced by its doping concentration and mobility through Equation (5.2).

$$\rho = {}^{1}/_{\sigma} = {}^{1}/_{\mu q n} \tag{5.2}$$

With the increasing thickness, the resistance of ZnMgO will increase, and the performance of CdTe solar cells can be hurt.

Same to the study on the influence of thickness, we should investigate the influence of doping concentration under different thicknesses. It can be expected that when the thickness of ZnMgO is big, the doping concentration can strongly influence the characteristics of CdTe solar cells. As discussed before, long doping concentration with a big thickness of ZnMgO layer can be harmful. However, if the thickness of ZnMgO is small, 5 nm as an example, the electrons can tunnel through ZnMgO layer. High doping and low doping of ZnMgO can both bring an ideal n^+-p junction structure and MRS structure, respectively. It will be interesting to compare which structure is better.

Using Figure 4.1 (b) as an example, under positive conduction band offset condition, the shape of the 'spike' is determined by the electron affinity and doping

concentration of ZnMgO. The height of the 'spike' is determined by the electron affinity according to Equation (1.2). The width of the 'spike is determined by the doping concentration since the depletion width, also energy difference between the Fermi level and conduction band of the window layer (ΔE_n), shown in Equation (5.3), has a relationship with the doping concentration.

$$\mathrm{n} = N_D = N_c \exp(^{-\Delta E_n}/_{kT}) \tag{5.3}$$

Here, N_c is the effective density state of the conduction band. *kT* is the thermal energy of electrons, which equals to 0.026 eV at room temperature. With the increase of doping concentration, the width of the 'spike' will decrease and the energy level of the conduction band of the window layer will shift down.

5.2 Simulated results

Firstly, two solar cells using ZnMgO, with a thickness of 10 nm and 200 nm, respectively, as the window layer is simulated. Simulated QE results of the two solar cells are provided in Figure 5.1. We can find that even the thickness of ZnMgO layer is enlarged by 20 times. The quantum efficiency of only shows a very limited decrease due to the reflection in this layer. The short-circuit current only reduces 0.27 mA/cm^2 from 26.12 mA/cm^2 to 25.85 mA/cm^2. This proves that the blue loss, even the optical loss in ZnMgO layer is negligible, which is different from the case using CdS as the window layer, shown in Figure 5.2, where the blue loss and can be significantly removed by reducing its thickness.

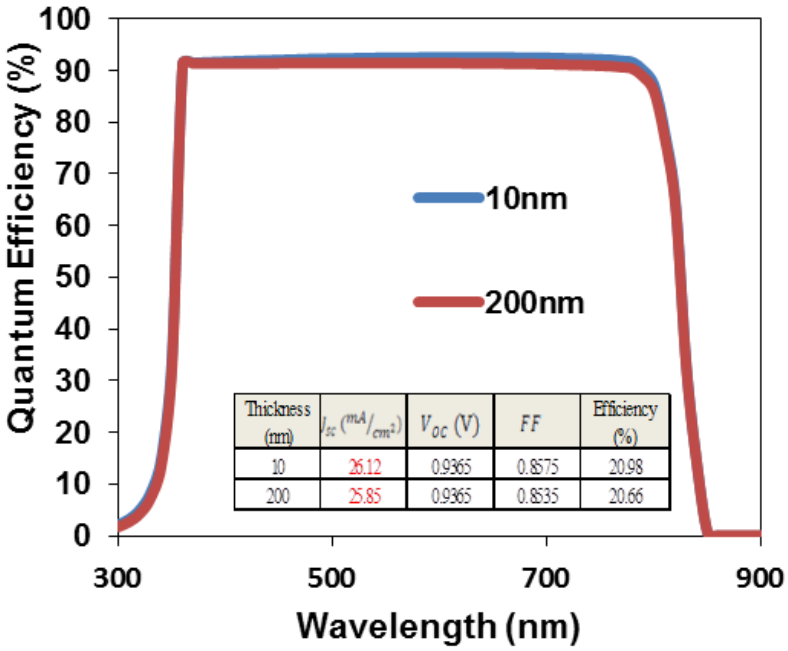

Figure 5.1 Simulated QE results on two different thickness of ZnMgO.

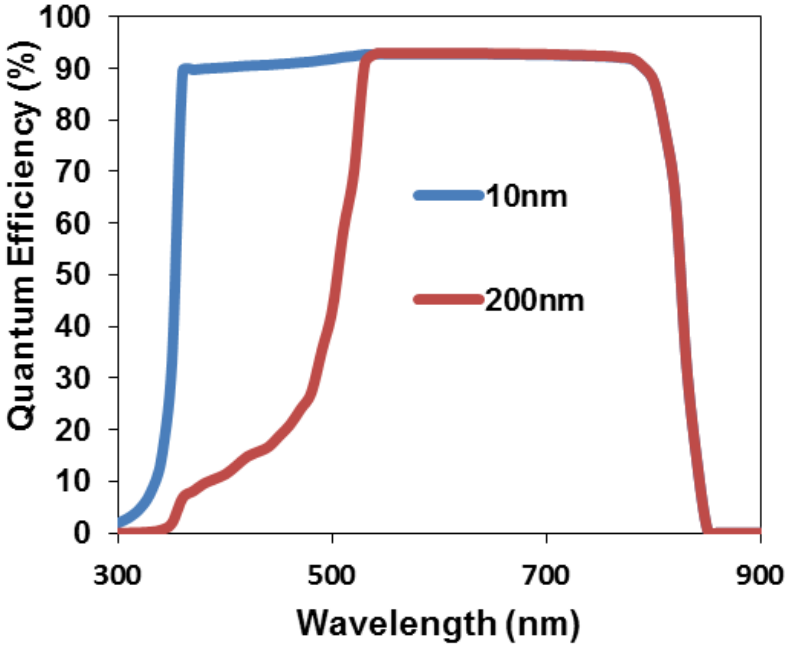

Figure 5.2 Simulated QE results on two different thicknesses of CdS.

3-D figures, shown in Figure 5.3, are plotted to depict the J-V performance, including open-circuit voltage; short-circuit current; fill factor; and efficiency, of CdTe solar cells as a function of the thickness at different doping concentrations of ZnMgO. The concluded influence of the thickness on the performance of CdTe solar cells with different structures is listed in Table 5.2.

When the doping concentration of ZnMgO layer is big, higher than 10^{17} cm^{-3}, in the case of n^{+}-p junction, the thickness shows almost negligible influence on the performance of CdTe solar cells as expected. The slight increase of the short-circuit current in the range of 10 to 50 nm indicates certain thickness is needed to play a role of buffer. Otherwise, the leakage current will lead to the decrease of short-circuit. Since SCAPS is a one-dimensional simulation program, the uniformity of the ZnMgO layer is unable to be taken into consideration during the simulation. This means the leakage current can be more severe in real applications. The decrease of short-circuit current when the thickness is bigger than 50 nm possibly comes from the recombination in the ZnMgO. Although this kind of decrease is limited, a too big thickness of ZnMgO is not desired even in n^{+}-p junction structures.

When the doping concentration of ZnMgO layer is smaller than 10^{15} cm^{-3}, in the case of MRS structure, the performance of CdTe solar cells drops down severely with the increase of the thickness. This meets our theoretical analysis since in CdTe solar cells with an MRS structure, the increasing thickness of the resistor (insulator) layer can impede the tunneling of the electrons across this layer and further harm the performance of the solar cells due to its high resistivity.

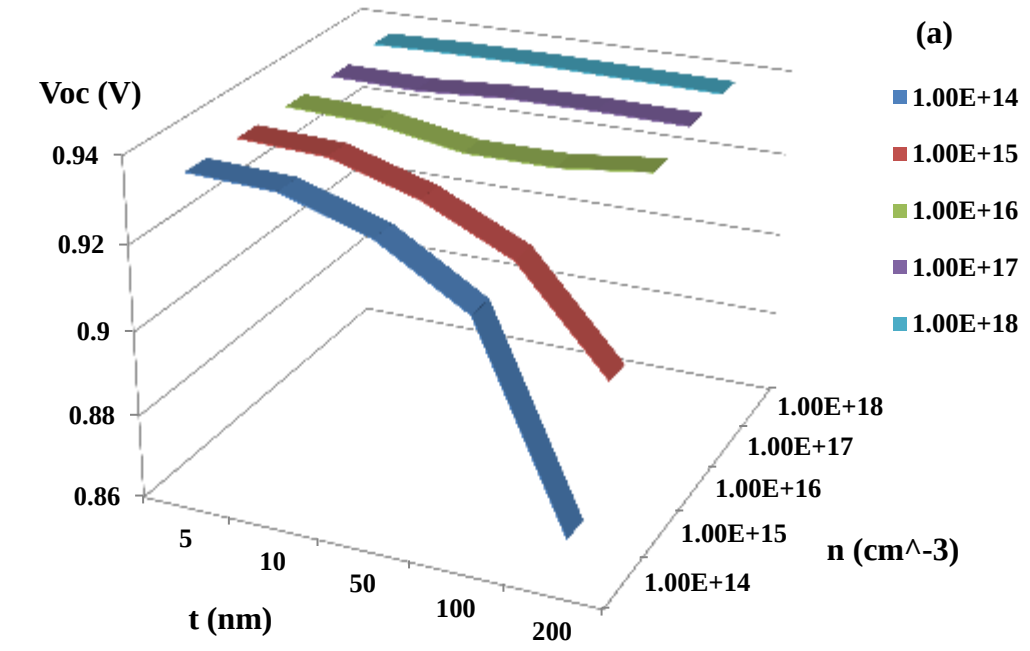

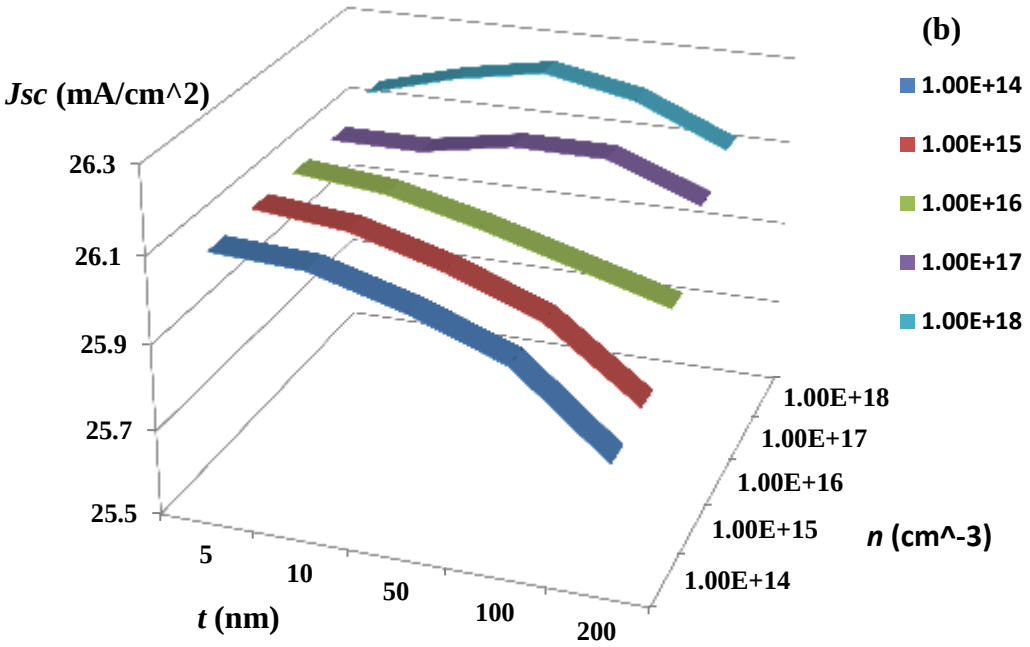

Figure 5.3 J-V performance of CdTe solar cells as a function of the thickness at different doping concentrations of ZnMgO. (Continued)
Note: (a) open-circuit voltage, (b) short-circuit current, (c) fill factor, (d) efficiency.

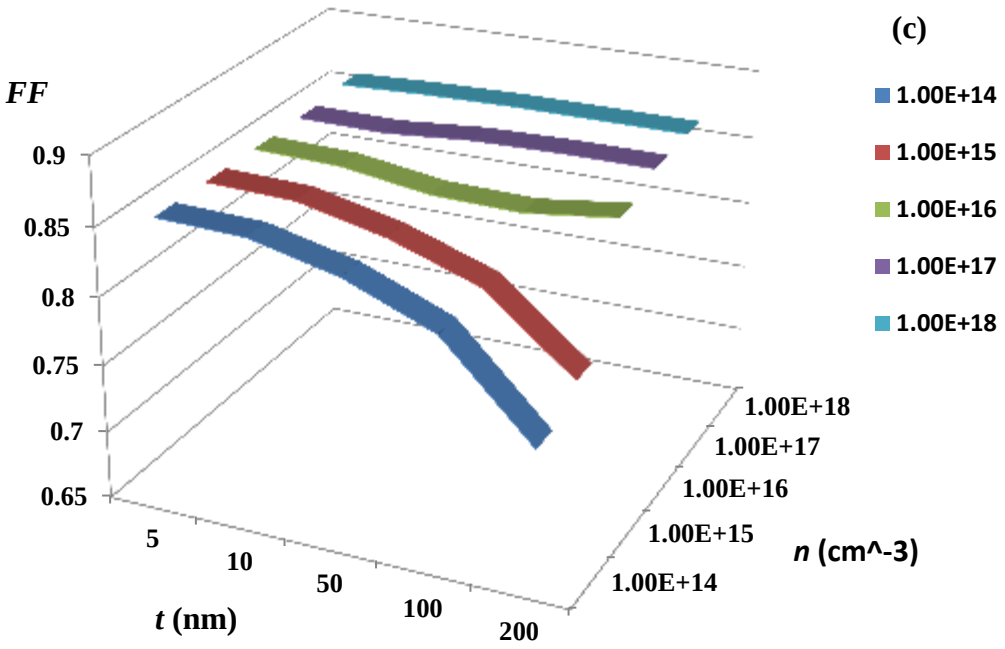

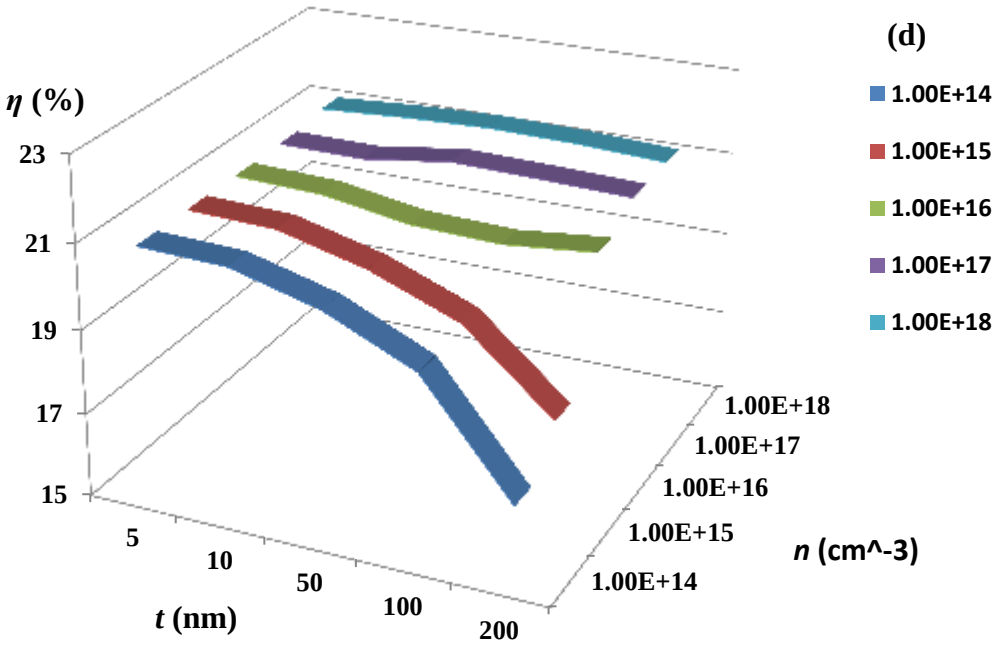

Figure 5.3 (Continued) J-V performance of CdTe solar cells as a function of the thickness at different doping concentrations of ZnMgO.
Note: (a) open-circuit voltage, (b) short-circuit current, (c) fill factor, (d) efficiency.

When the doping concentration of ZnMgO layer is at the level of 10^{16} cm^{-3}, in the case of n^+-n-p structure, a mixture of n^+-p junction structure and MRS structure, the performance, except short-circuit current, of CdTe solar cells drops down before the thickness of ZnMgO reaches 100 nm, but then raise up in the range 100 nm to 200 nm. The reason is quite clear. When the thickness of ZnMgO is smaller than 100 nm, the structure of CdTe solar cells is MRS structure since x_n, calculated from Equation (5.1), is 100 nm when n is 10^{16} cm^{-3}. As an MRS structure, the performance of the solar cells goes down with the increasing thickness of the resistor layer. When the thickness of ZnMgO is bigger than 100 nm, an n^+-p junction structure is formed between ZnMgO window layer and CdTe absorber layer. Thus, the influence of the thickness of ZnMgO layer becomes negligible and a slight enhancement on the performance of CdTe solar cells is possible.

Table 5.2 The influence of the Thickness of ZnMgO at Different Structure of CdTe Solar Cells from the Simulated Results

Structure of CdTe solar cells	**Influence of the thickness of ZnMgO layer**
n^+-p junction	Almost negligible influence
n^+-n-p	The performance of CdTe solar cells drops down with the increasing of the thickness at first, then becomes negligible after an n-p junction is formed
MRS	The performance of CdTe solar cells drops down with the increasing of the thickness

Compared with other researchers' publication [47], there are some mismatches between our simulated results and their experimental results. One possible reason is that the buffer function of the window layer cannot be properly reflected in the SCAPS

program. An example is when we remove the window layer, making the TCO layer direct contact with the CdTe layer, the simulated J-V results make almost no difference with the one that a window layer is added. This is definitely not the truth, since the SCAPS does not allow us to simulatie the purported MRS structure with n = 10^21 cm^-3, the real doping of the TCO. Instead, we use n = 7.8 x 10^17 cm^-3, which makes the structure equivalent to n+-p solar cell. Experimentally, the TCO layer can make unfavorable band alignment with CdTe, from a combination of electron affinity, charged defects and degenerated doping. Also, the TCO layer with degenerated doping cannot be suitably simulated in SCAPS according to the E-mail discussion between the author of this dissertation and Dr Burgelman, from University of Gent, the inventor of the SCAPS simulation program. Thus, we have to rely on experimental data to further investigate the performance of CdTe solar cell with different thicknesses of the window layer.

3-D figures, shown in Figure 5.4 are also plotted to depict the J-V performance, including open-circuit voltage; short-circuit current; fill factor; and efficiency, of CdTe solar cells as a function of the doping concentration at different thicknesses of ZnMgO.

The results are within our expectation. At low thicknesses of ZnMgO, smaller than 10 nm, the doping concentration has almost no influence on the performance of CdTe solar cells except a minor increase when the doping concentration is 10^{18} cm^{-3}. This means n-p junction structure does not have superior performance over MRS structure in the simulation. But a ZnMgO layer smaller than 10 nm may bring uniformity problems, which means leakage current can be large when MRS is in practical use. The influence of the doping concentration becomes more severe with the increase of thickness since for an n-p junction, higher doping in the ZnMgO layer brings the advantage of a larger built-in

voltage by reducing the value of ΔE_n according to Equation 4.11. Also higher doping means lower resistivity of ZnMgO layer, which is beneficial to photo-generated electrons.

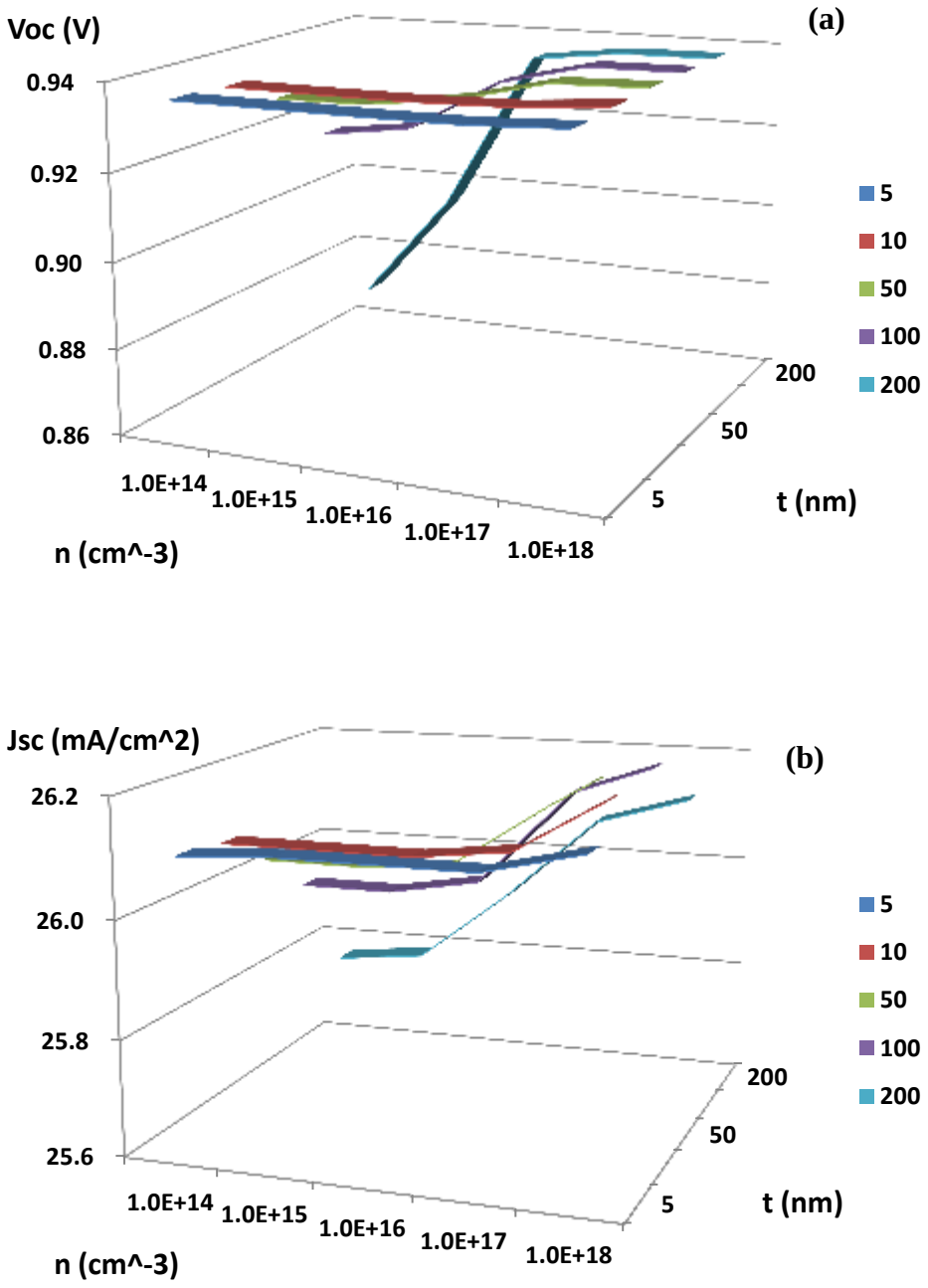

Figure 5.4 J-V performance of CdTe solar cells as a function of the doping concentraion at different thicknesses of ZnMgO. (Continued)
Note: (a) open-circuit voltage, (b) short-circuit current, (c) fill factor, (d) efficiency.

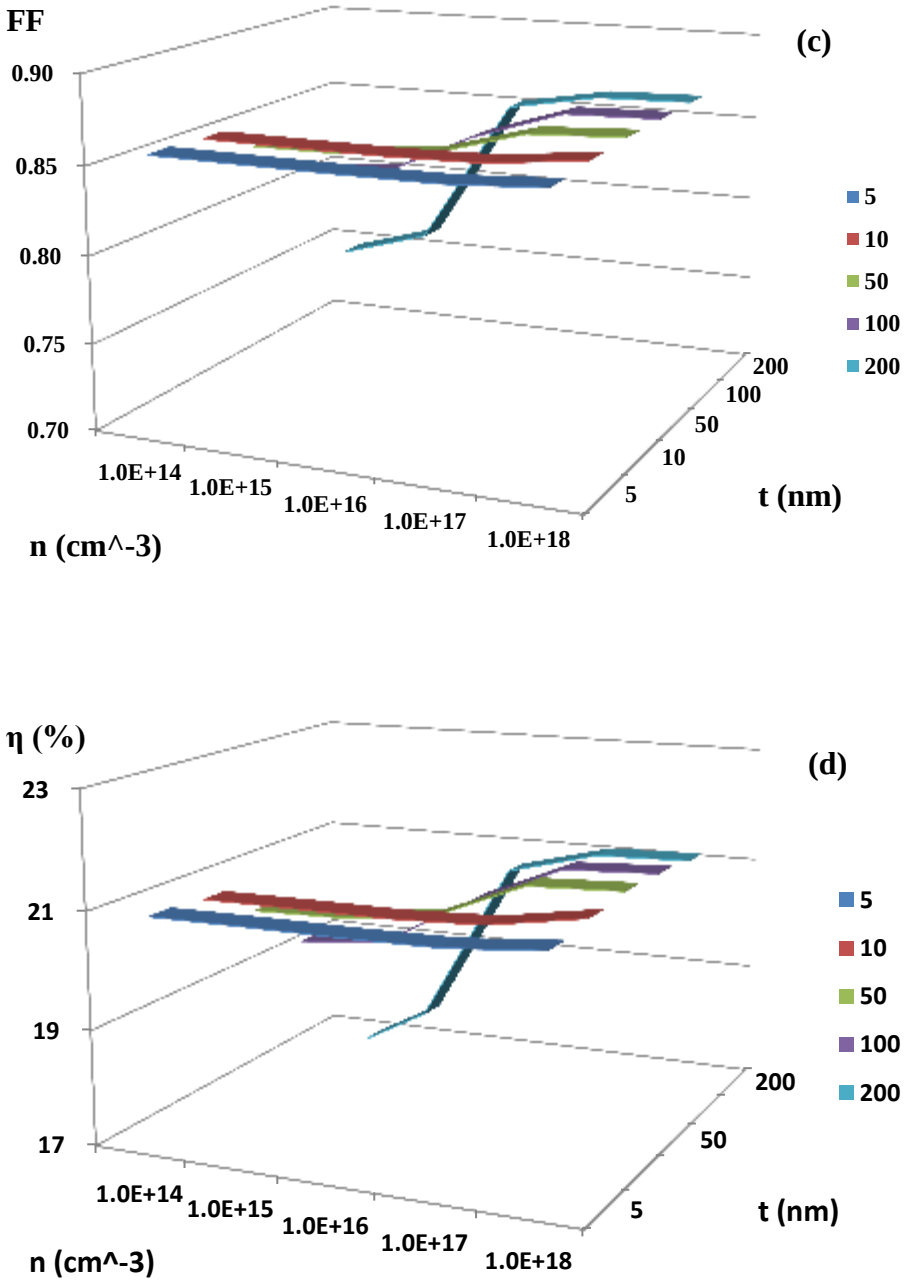

Figure 5.4 (Continued) J-V performance of CdTe solar cells as a function of the doping concentraion at different thicknesses of ZnMgO.
Note: (a) open-circuit voltage, (b) short-circuit current, (c) fill factor, (d) efficiency.

The influence of the doping concentration of the ZnMgO layer on the intra-band tunneling is also simulated. A CdTe solar cell is configured with a 0.4 eV conduction band

offset. From the simulated results in Chapter 4, the performance of CdTe solar cells will start to degrade when the conduction band offset is 0.4 eV when the intra-band tunneling is excluded from the simulation. However, the simulated solar cells still work well when the conduction band offset is included. So, 0.4 eV is a good value for conduction band offset to simulate the influence of doping concentration of ZnMgO on the intra-band tunneling. ZnMgO layers with four doping concentrations, 10^{14} cm^{-3}, 10^{-16} cm^{-3}, 10^{17} cm^{-3}, and 10^{18} cm^{-3}, respectively, are simulated and their corresponding J-V performance is plotted in Figure 5.5. The conduction band diagrams of the four simulated solar cells are also plotted, as Figure 5.6 shows.

From both Figure 5.5 and Figure 5.6, we can find that when the doping concentration is 10^{14} cm^{-3}, ZnMgO layer fails to form an n-p junction, (the conduction band of ZnMgO layer is a straight line with no band bending) and the distance for the electrons to make the intra-band tunneling is same as the thickness of ZnMgO, 70 nm in this simulation, which is too big for electrons to tunnel through this layer. Thus, even with intra-band tunneling included, the performance of the CdTe solar cell is still very weak and its fill factor is extremely low with a kink. This again proves that a big conduction band offset acts as a secondary barrier for the photo-generated electrons and is the origination of the kink in J-V curves. When the doping concentration reaches 10^{16} cm^{-3}, ZnMgO layer starts to form an n-p junction with CdTe, (band bending starts to exist), but due to its relatively low doping, the distance for the electrons to tunnel through the ZnMgO layer is still very big. The mechanism of intra-band tunneling cannot help improve the performance of CdTe solar cells too much. Thus, J-V characteristics of CdTe solar cells only improve very little and the kink still exists with a low fill factor. It is not until the

doping concentration of ZnMgO layer reaches 10^{18} cm^{-3} that the distance of the electrons to tunnel through the ZnMgO layer becomes significantly decreased. Shown from Figure 5.6 (d), the distance for the electrons to make the intra-band tunneling at the energy level of 1.1 eV (+0.2 eV conduction band offset) is very small, less than 5 nm, which means the possibility for the intra-band tunneling to happen increases a lot and the performance of the CdTe solar cell enhances dramatically.

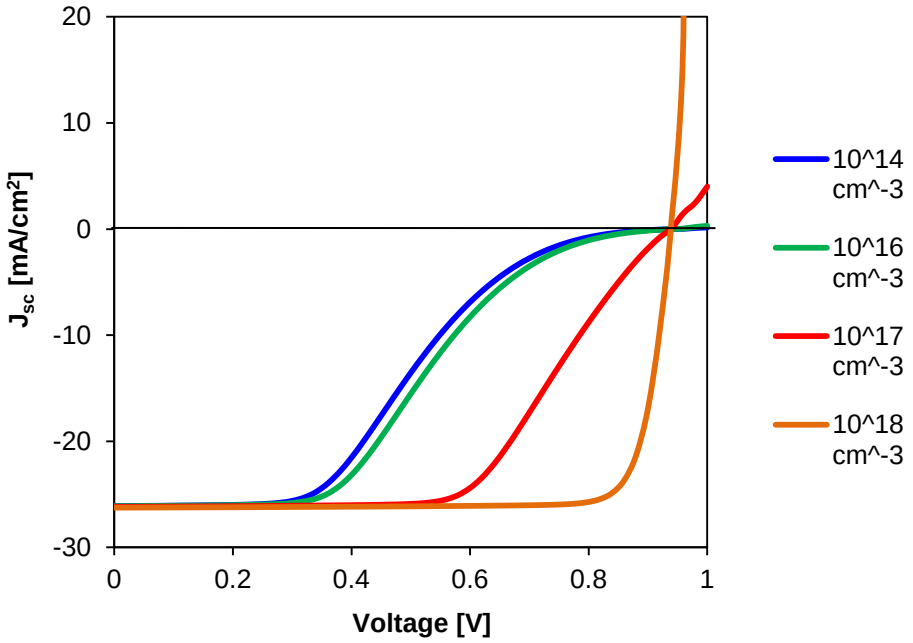

Figure 5.5 J-V performance of the simulated CdTe solar cell with different doping concentration of ZnMgO.

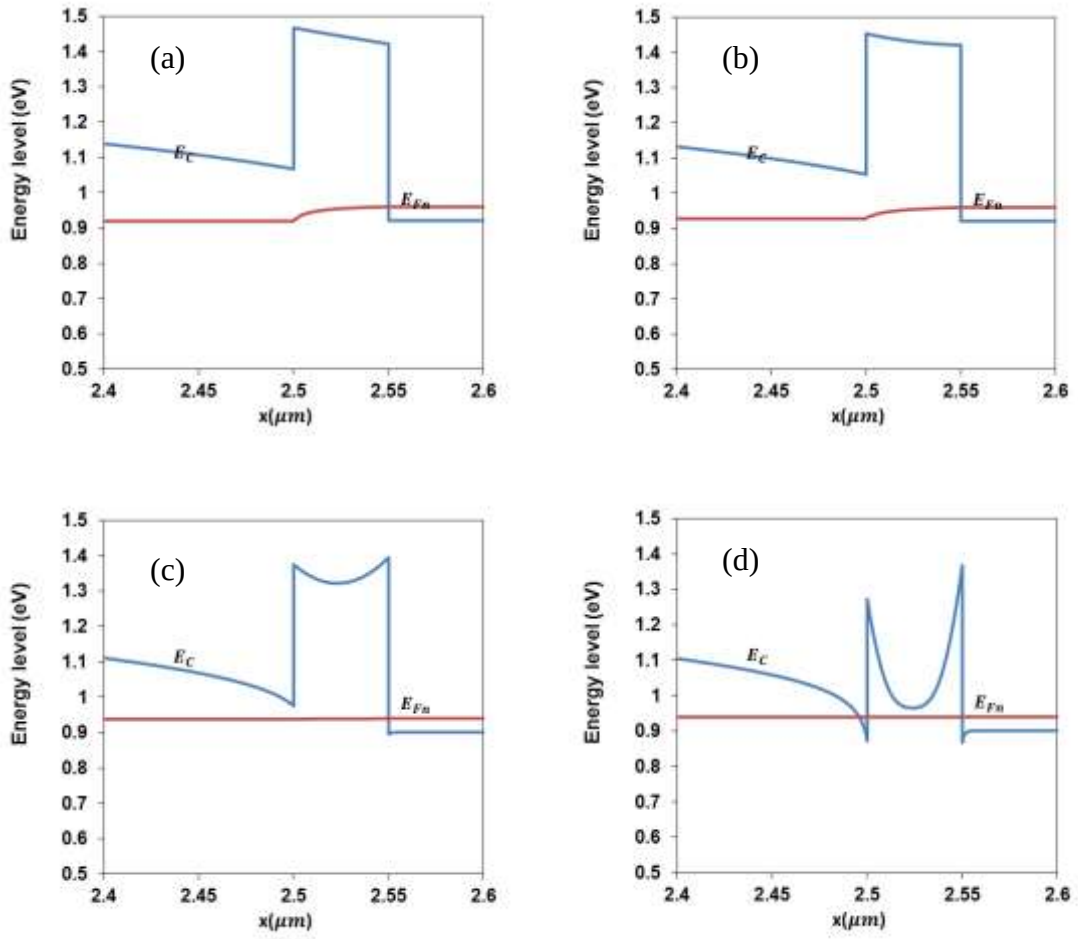

Figure 5.6 Conduction band diagram of the simulated CdTe solar cells.
Note: (a) The doping concentration of ZnMgO is 10^{14} cm^{-3}, (b) The doping concentration of ZnMgO is 10^{16} cm^{-3}, (c) The doping concentration of ZnMgO is 10^{17} cm^{-3}, (d) The doping concentration of ZnMgO is 10^{18} cm^{-3}.

From the simulated results, when the thickness of ZnMgO layer is small, CdTe solar cells with an n-p junction does not have better performance than that with an MRS structure. The influence of the doping concentration for ZnMgO on CdTe solar cells becomes more severe when the thickness ZnMgO layer becomes bigger. Besides, doping concentration can significantly influence the intra-band tunneling and high doping is demanded to achieve good performance of CdTe solar cells when the conduction band offset is big. Considering the practical difficulties to fabricate an MRS structure using

ZnMgO, and the uniformity problems of a thin ZnMgO layer, an n-p junction structure is better for CdTe solar cells when using ZnMgO as the window layer. Then, high doping seems to be the first choice. However, the simulated results also need experimental certificate.

5.3 Experimental Results

To experimentally investigate the influence of the thickness of ZnMgO layer, four batches of ZnMgO layer deposited on FTO are processed to solar cells. All the conditions during the film deposition are same except the deposition time. Thus, besides the thickness, other properties of the ZnMgO thin films are approximately considered the same. The measured thickness of these four batches of ZnMgO layer is 10 nm, 20 nm, 50 nm and 130 nm, respectively. The measured J-V results are listed in Table 5.3 and corresponding J-V curves are plotted in Figure 5.7.

The extreme low fill factor comes from a combination of a big conduction band offset for our center's CdTe solar cells, 0.42 eV as estimated, and the processing on the back contact. Since there is no clear tendency on the fill factor, we should not take it into consideration to investigate the influence of ZnMgO layer's thickness. Regardless the fill factor, the open-circuit voltage and short-circuit current of the fabricated CdTe solar cells shift with the increasing of the thickness for ZnMgO layer. This means the doping concentration of ZnMgO layer is not high, and our CdTe solar is in an MRS structure. The slightly increase of open-circuit, short-circuit when the thickness of ZnMgO is increased from 10 nm to 20 nm shows that certain thickness is needed for the window layer in order

to play a role of buffer. A too thin ZnMgO can sacrifice its uniformity. With the thickness of ZnMgO continues increasing, the J-V performance of CdTe solar cells starts degrading because of the increasing resistance of ZnMgO (Resistor) layer. The overall experimental results on the influence of the thickness for ZnMgO layer are quite same with the results from Colorado State University [47]. The optimized thickness for ZnMgO layer should be between 20 nm to 50 nm. 40 nm is regarded as a best choice.

Table 5.3 The Measured J-V Results for CdTe Solar Cells with Different Thickness of ZnMgO

Thickness nm	**V_{OC}** *V*	**J_{SC}** *mA/cm²*	**FF**	**Efficiency** %
10	0.823	26.59	0.478	10.46
20	0.83	27.29	0.4127	9.36
50	0.828	25.14	0.4015	8.40
130	0.717	23.58	0.2691	4.55

To experimentally investigate the influence of the doping concentration of ZnMgO, three batches of ZnMgO layer deposited on FTO are processed to solar cells. All the conditions during the film deposition are same except the Ar/O_2 ratio in the chamber. The deposited ZnMgO thin films are characterized by Hall measurement. The results all shown in Table 5.4. Although there is difference between the thickness and mobility of the three deposited ZnMgO layers, the influence of them can be ignored compared with the influence of the doping concentration. Besides, ZnMgO layers made in our center has a 15% atomic percent, leading to a 0.42 eV conduction band offset. Hence, the influence of the doping concentration on the intra-band tunneling can be investigated. The measured J-V curves of these three CdTe solar cells are shown in Figure 5.8. Since all the cells we have

made have low efficiency, our argument about the dependence of efficiency on thickness seems weak, since there are other factors affecting the cells' efficiency.

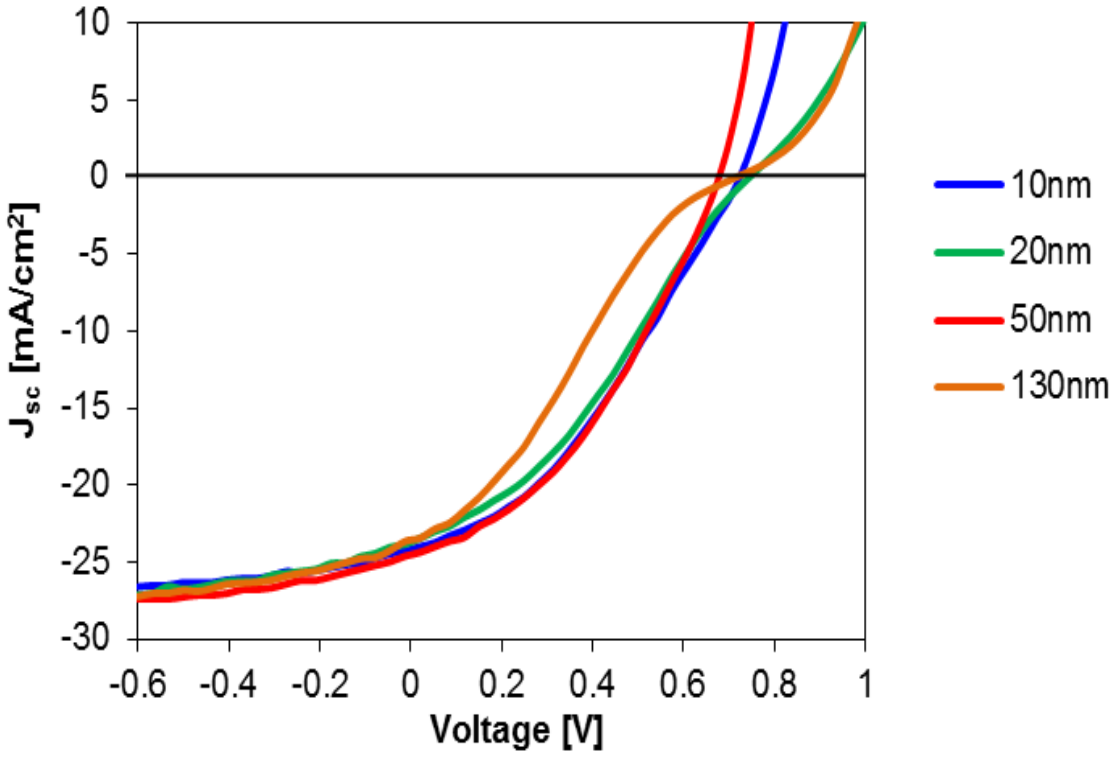

Figure 5.7 The measured J-V curves of CdTe solar cells with different thickness of ZnMgO.

Table 5.4 The Hall Measurement Results of the Deposited ZnMgO Samples

Sample #	**Thickness** *nm*	**Doping concentration** */cm*^{3}	**Mobility** cm^2/V.s
1	26	3*10^{15}	2
2	30	1*10^{17}	13
3	37	1*10^{18}	18

From the measured J-V curve, a kink exists when the doping concentration of ZnMgO layer is small, leading to a low fill factor. With the increasing of the doping

concentration, kink finally disappears and the J-V performance of CdTe solar cells becomes better. This meets the theoretical model of intra-band tunneling that a high doping ZnMgO layer can increase the possibility for the electrons to tunnel through the 'spike', caused by a big conduction band offset, with both thermionic emission and field emission. High doping can tolerate a bigger value of conduction band offset. However, even with a high doping concentration of 10^{18} cm^{-3}, the fabricated CdTe solar cell's fill factor is still too low, compared with the ideal J-V curve in Figure 5.5. Thus, the processing methods for the CdTe solar cell in our lab still need to be improved.

Take both simulated and experimental results, also other researches' work into consideration; following conclusions on the influence of the thickness and doping concentrations on the performance of CdTe solar cells are made. Doping concentration has a strong influence on the performance of CdTe solar cells only when the thickness is relatively big and it determines the structure of CdTe solar cells. High doping leads to an n^+-p junction structure whereas low doping leads to an MRS structure. Between them, we can call it n^+-n-p structure. High doping with an n^+-p junction structure can tolerate a bigger conduction band offset, and the thickness of ZnMgO only needs to bigger than the electron depletion width in this layer. Low doping with an MRS structure requires the thickness of ZnMgO as small as possible. But certain thickness for ZnMgO layer must be maintained to grantee its function as a buffer, meaning an MRS structure may bring problems in practical applications. An n^+-p junction structure is preferred to CdTe solar cells. The recommended thickness and doping concentration for ZnMgO is 40 nm and 10^{18} cm^{-3}, respectively. Sample # 3 in Table 5.4 appears to satisfy the specification for optimal ZMO.

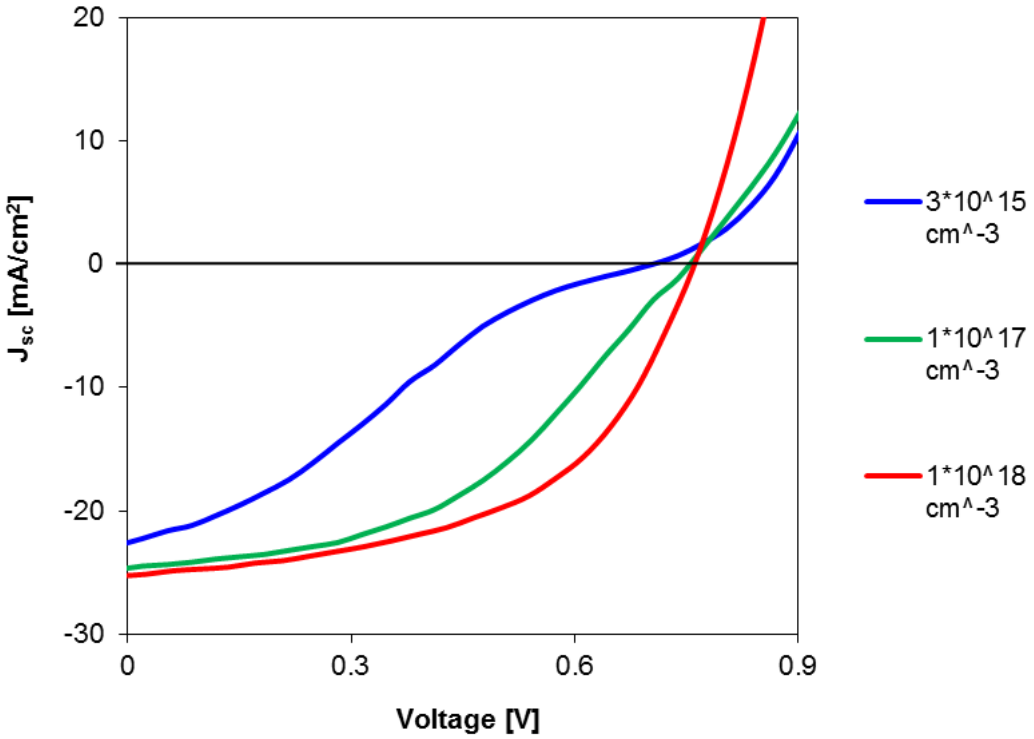

Figure 5.8 Measured J-V performance of CdTe solar cells with different doping concentration of ZnMgO.

CHAPTER 6

THE INFLUENCE OF TCO LAYER

The most important characteristics for TCO materials are their optical and electrical properties. In this dissertation, a simple and preliminary model is provided that the thickness of TCO layer is related to its optical and electrical properties, further the whole performance of CdTe solar modules.

For a TCO layer, light absorption is proportional to the thickness according to Equation (6.1).

$$\mathrm{T} = (1 - \mathrm{R})\exp(-\alpha \mathrm{t}) \tag{6.1}$$

In this equation, T, A and R is the transmittance, absorption, reflectance of the TCO layer, respectively. α is the absorption coefficient, t is the thickness of the TCO layer and αt together is the optical energy loss (OEL) in the TCO layer, which means the thickness of TCO should be reduced considering from the optical loss.

However, the electrical energy loss for the TCO layer is reverse proportional to its thickness. The electrical energy loss (EEL) for TCO can be written as Equation (6.2).

$$\mathrm{EEL} = J^2 R_{sh} \tag{6.2}$$

J is the current density for CdTe solar cells at the max output power, which is just smaller than the short-circuit density and can be treated equal to 20 mA/cm^2. R_{sh} in this equation is the sheet resistance for the TCO layer. The sheet resistance of TCO layer is reverse proportional with the thickness as Equation (6.3) indicated.

$$R_{sh} = {}^{\rho}/_{t} \tag{6.3}$$

ρ is the resistivity of the TCO layer and can be expressed as Equation (5.2) shows. This means that the thickness of TCO layer should be increased considering the electrical energy loss.

The total energy loss (TEL) is the sum of optical energy loss and electrical energy loss in the TCO layer and can be written as Equation 6.4.

$$\mathrm{TEL} = \mathrm{OEL} + \mathrm{EEL} = \alpha t + {J^2}/{\mu q n t} \tag{6.4}$$

Assume the term ${J^2}/{\mu q n}$ is β, then to minimize the total energy loss, $\frac{\mathrm{d(TEL)}}{dt}$ should be equal to 0 and the expression for the optimized thickness of TCO can be derived as Equation 6.5 indicates.

$$t = \sqrt{\frac{\beta}{\alpha}} = \frac{J}{\sqrt{\alpha \mu q n}} \tag{6.5}$$

The absorption coefficient of TCO can be measured by FILMETRICS and the doping concentration and mobility of TCO can be achieved by Hall measurement. Putting the measured values into Equation (6.5), the theoretical optimized thickness of TCO in this model can be calculated.

One cadmium stannate (CTO) and one (Aluminum doped ZnO) AZO sample are deposited by the HCSS in our lab. The deposited samples are subsequently characterized by FILMETRICS and Hall measurement. The measured optical and electric properties of the samples are shown in Table 6.1.

Putting the values into Equation (6.5), the calculated optimized thickness for CTO and AZO samples is 61 and 94 μm, respectively. However, this number is definitely too big and unreliable, which means the model needs to be modified, especially for the electrical loss part.

Table 6.1 The Measured Optical and Electrical Properties of the TCO Samples

Sample	**t** nm	**α** /cm	**n** /cm^3	**μ** cm^2/V.s
CTO	459	$3.97*10^3$	$4.08*10^{20}$	41.95
AZO	481	$1.45*10^3$	$6.00*10^{20}$	33.07

Then an improved model is released [75]. The schematic diagram of the current in the TCO layer of solar cell modules is shown in Figure 6.1. The current at the boundary of the grid is equal to:

$$I = JLW \tag{6.6}$$

J is the current density when the maximum output power is achieved. L, W is the length and width of the grid, respectively. Since current in the grid is linear in terms with the location, then the current at a certain place I(x) equals to:

$$I(x) = JxL \tag{6.7}$$

The resistance at a certain place R(x) equals to:

$$R(x) = \rho\frac{dx}{tL} = R_{sh}\frac{dx}{L} \tag{6.8}$$

The power loss at a single place P(x) then can be derived as Equation 6.9.

$$P(x) = I(x)^2R(x) = J^2x^2L\frac{dx}{\mu qnt} \tag{6.9}$$

By integrating x from 0 to W, the total electrical power loss P then can be calculated and is shown in Equation 6.10.

$$P = \frac{1}{3}\frac{J^2w^3L}{\mu qnt} \tag{6.10}$$

Thus, the electrical power loss in this model is still reverse proportional with the thickness of TCO. Then the value of β is the ration of electric power loss to the incoming power, which is equal to:

$$\beta = \frac{1}{3}\frac{J^2 w^2}{E\mu q n} \tag{6.11}$$

Here, *E* is the irradiance, and is 100 mA/cm^2 at one sun condition.

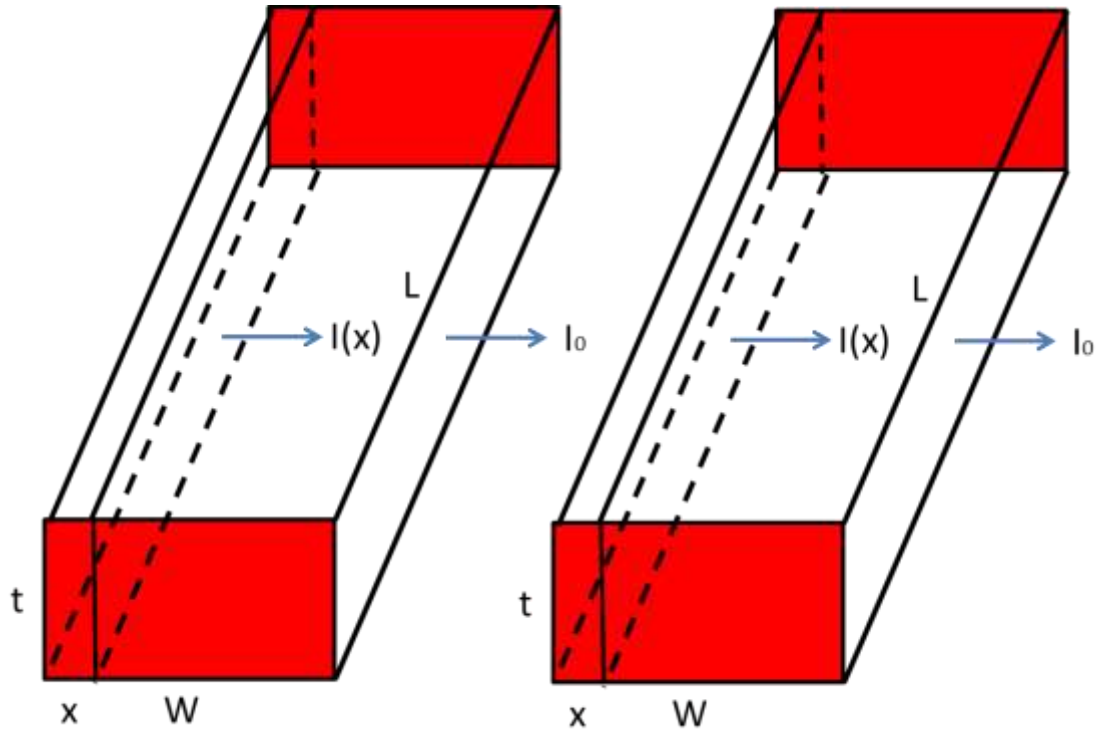

Figure 6.1 The schematic diagram of the current in the TCO layer of the solar cell module.

Now putting all the values into Equation 6.11, the new β value and the optimized thickness of TCO layer can be achieved. The optimized thickness for CTO and AZO is 202 nm and 311 nm, respectively. The results are more reasonable now and quite match the data in the real application.

To further investigate the influence of thickness of TCO, SCAPS simulation is done using the optical and electrical data of our AZO sample. However, simulated results show that the J-V performance is exactly same when the thickness of TCO is 100 nm and

500 nm, respectively. The reason is that the electrical loss only happens at solar cell modules. It will not happen in solar cells. Thus, the simulation program is unable to reflect.

CHAPTER 7

CONCLUSION

7.1 Some Novel Ideas on the Front End

Before going to the final conclusion of this dissertation, some novel ideas based on computer simulation are presented here on the window layer of the CdTe solar cell.

The first one is replacing a single window layer structure with an electrode-buffer two-layer structure. Practically, some of the commercial TCO glss products are coated with a thin hgh resistant transparent (HRT) layer, which serves as the window-buffer. As mentioned in the previous chapters, it looks that the window layer is better to be highly doped and plays a role of both buffer and electrode. However, a two layer structure may perform better and is included in one of First Solar's patent [76]. Then a CdTe solar cell with the following structure is simulated: TCO/ ZnMgO (low doping)/ ZnMgO (high doping)/ CdTe/ Cu. The thickness of low doping ZnMgO layer and high doping ZnMgO layer is 20 nm each. The doping for them is 0 and 10^{18} cm^{-3}, respectively. The simulated J-V results are plotted in Figure 7.1. From the simulated results, the performance of CdTe solar cell can be enhanced by adjusting the conduction band offset between the high doping ZnMgO layer and low doping ZnMgO layer. A possible reason is that the low doping ZnMgO layer can be treated as an insulator and in that case the doping conduction band offset between the two ZnMgO layers becomes dominant for the performance of CdTe solar cells. The corresponding conduction band diagram for the simulated solar cell is also plotted, shown in Figure 7.2.

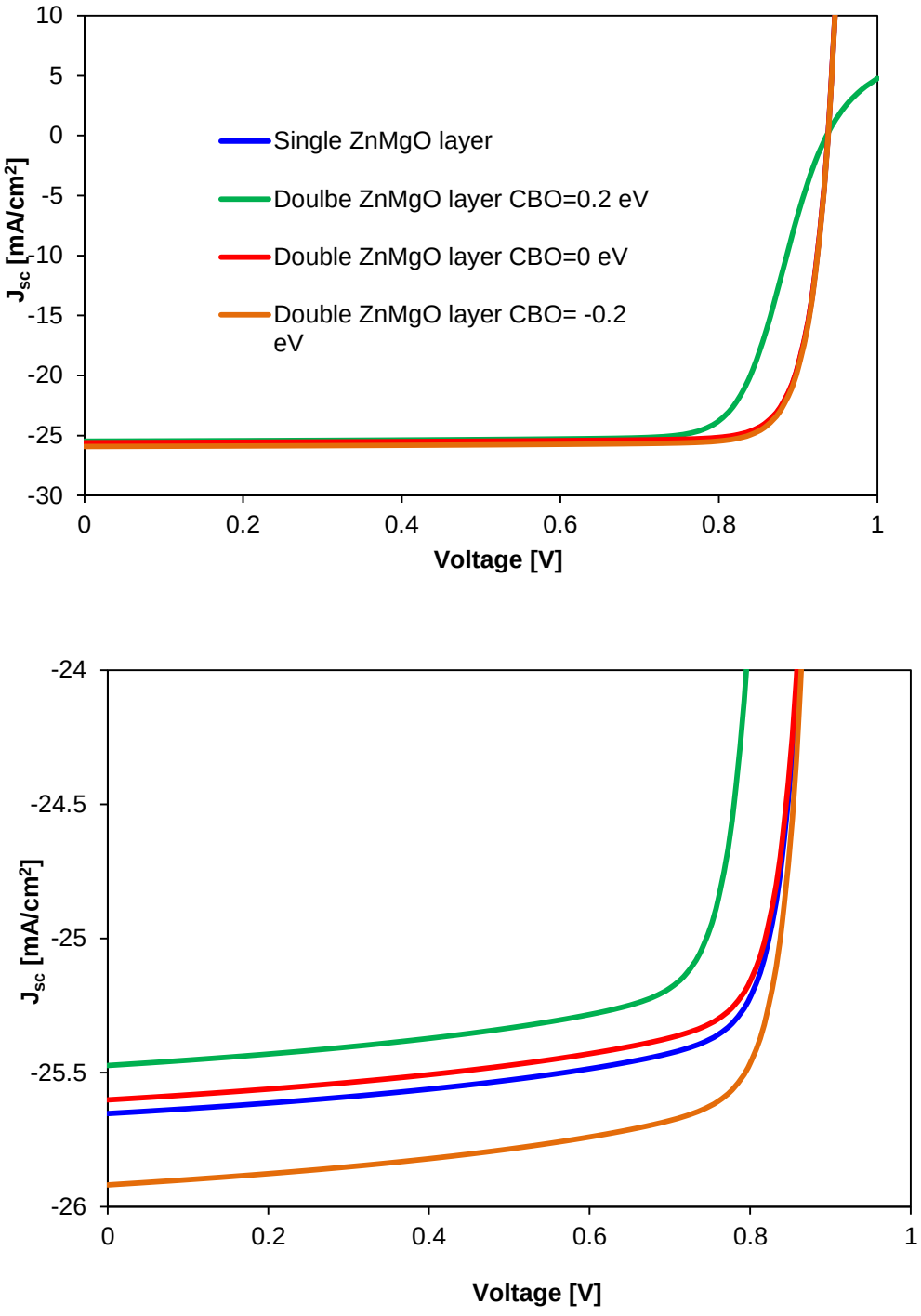

Figure 7.1 Simulated J-V results with different structures and different conduction band offset for CdTe solar cells.

Note: The data indicates that there are only minor differences in short-circuit of the cells.

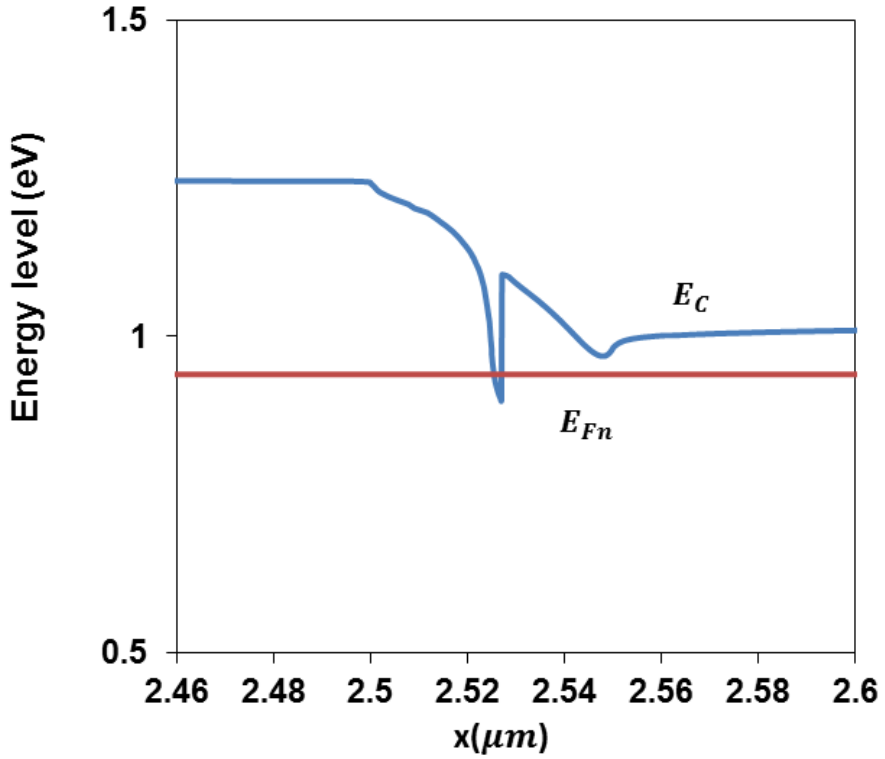

Figure 7.2 The conduction band diagram of the simulated CdTe solar cells with two ZnMgO layers.

The second one is trying graded doping for window layers. The reason to do graded doping is our hope to generate a drift force to the movement of photo-generated electrons so that the short-circuit current can be enhanced. Thus, the ZnMgO layer's doping is changed from uniform 10^{18} cm^{-3} to linear graded doping in the range of 10^{18} cm^{-3} to 0. However, simulated results indicate that the performance of CdTe solar cell does not improve and the efficiency is only increased by 0.05%, which is negligible.

7.2 Conclusions on the Front End

Performance comparison of CdTe Cells processed at CNBM Center, using different kinds of materials as the window layer, and CSU are listed in Table 7.1. As demonstrated by the 14% CdTe solar cell using the old technology of CdS window layer, as well as the dark current data of Figure 1.5 and 4.11, we have mastered the basic techniques of fabricating CdTe solar cells at the CNBM Center. After switching to the new technology using windows of wider band gap materials, such as CdSO, SnMgO, and most importantly ZMO, however, the efficiency of our cells keep hovering around 10%. Since our best and typical CdTe solar cell using wide band gap windows have reasonable short-circuit current and open-circuit voltage, as well as good performance under dark, we tentatively conclude that the primary difficulty we have encountered is low fill factor, which is only around 60% of the fill factor of the good CdTe cell with the ZMO window layer reported by CSU. As shown by Figure 1.5 and 4.11, the photocurrent density of the CNBM Center's CdTe cells starts to go down noticeably around the output voltage of 0.4 V. The difficulty of collecting the photo-current may be caused by three deficiencies in our technology.

First, we have not learned to process the ZMO window layer with proper conduction band offset and doping. As shown in Figure 4.1 and 5.1, the electron drift current generated by solar illumination faces the energy barrier of the conduction band offset. It is the intra-band tunneling that facilitates the overcoming of the barrier. The intra-band tunneling, however, is hindered by the increase of the output voltage and reduction of the band bending of CdTe as well as the ZMO. Therefore, too high conduction band offset and too low doping of ZMO may cause the reduction of fill factor.

Second is the lack of electron reflection at the back contact since we have not succeeded in incorporating Se in the CdTe absorber.

Third is the poor p-type Ohmic contact at the back. After circulating through the external circuit, the electrons must be recombined with the holes coming out of the back of the CdTe. It is unfortunately beyond the scope of this dissertation to address and resolve the three issues experimentally.

Table 7.1 Performance Comparison of CdTe Cells Processed at CNBM Center and CSU

Window Layer Source	**CdS** NJIT	**ZMO** NJIT	**TMO** NJIT	**ZMO** CSU
V_{OC} (V)	0.816	0.836	0.76	0.863
J_{SC} (mA/cm^2)	23.2	25.9	23.85	26.8
FF	0.741	0.431	0.592	0.792
η (%)	14.0	9.3	10.74	18.3

Both the simulated and experimental results show us the following conclusion on the window layer. Wider band gap materials have been proved to yield a superior performance of CdTe solar cells compared with the traditional CdS mainly due to the removal of blue loss. ZnMgO is an ideal candidate and is the material used in this dissertation to optimize the window layer. The Mg content must be precisely controlled not for the changing of band gap, but for the adjusting of the conduction band offset. A small positive value for the conduction band offset is desired for the purpose of reducing surface recombination so that the performance of CdTe solar cells can be enhanced. However, a too big value for the conduction band offset is not suitable because it can act as a secondary barrier for the photo-generated electrons and destroy the solar cells, especially when the

doping concentration of ZnMgO layer is not high enough. The doping concentration of ZnMgO layer determines the structures of CdTe solar cells and its influence becomes severe with the increasing of thickness. When ZnMgO is highly doped, bigger than 10^{17} cm^{-3}, the CdTe solar cell is an n^{+}-p junction structure, the mechanism of intra-band tunneling can help the electrons tunnel through the 'spike', which is caused by a big value of conduction band offset; also the influence of the thickness is negligible. When ZnMgO is low doped, the structure of CdTe solar cells becomes MRS, small thickness is helpful for the electrons to tunnel through the layer directly and the increasing thickness of the layer can be harmful. But the uniformity problems for such a small thickness may drop down the performance of CdTe solar cells. The final conclusion of the optimized window layer is listed in Table 7.1. Some novel ideas on the optimization of the window layer are also mentioned and discussed, but may not be useful for CdTe solar cells.

The optimized thickness of TCO layer in CdTe solar cell modules is also theoretically calculated. The optimized thickness of CTO and AZO achieved from our model is 202 nm and 311 nm, respectively.

Table 7.2 The Concluded Optimized Parameters of the Window Layer for CdTe Solar Cells

Material	x %	E_g eV	ΔE_C eV	t nm	n cm^{-3}
$Zn_{1-x}Mg_xO$	10	3.5	0.3	40	$1*10^{18}$

REFERENCES

[1] "Photovoltaics Report", Fraunhofer ISE, 12 July 2017, Retrieved from https://www.ise.fraunhofer.de/content/dam/ise/de/documents/publications/studies/Photovoltaics-Report.pdf.

[2] M. Green, K. Emery, Y. Hishikawa, W. Warta, E. Dunlop, D. Levi, and A. Ho-Bailie, Prog. Photovolt. Res. Appl. 25, 3 (2017).

[3] G. Fonthal, L. Tirado-Mejia, J. Marin-Hurtado, H. Ariza-Calderon, and J. Mendoza-Alvarez, J. Phys. Chem. Solids 61, 579 (2000).

[4] X. Mathew, J. Mater. Sci. Lett. 21, 529 (2002).

[5] C. Su, J. Appl, Phys. 103, 084903 (2008).

[6] M. Lourenco, Y. Yew, K. Homewood, K. Durose, H. Richter, and D. Bonnet, J. Appl. Phys. 82, 1423 (1997).

[7] Y. Yoon, J. Chae, A. Katzenmeyer, H. Yoon, J. Schumacher, S. An, A. Centrone, and N. Zhitenev, in proceedings of EU Photovoltaic Solar Energy Conference and Exhibition (2015).

[8] W. Shockley and H. Queisser, J. Appl. Phys. 32, 510 (1961).

[9] A. Mohamed, J. Appl. Phys. 113, 093105 (2013).

[10] "Best Research-Cell Efficiencies", NREL, Retrieved from https://www.nrel.gov/pv/assets/images/efficiency-chart.png.

[11] M. Imamzai, M. Islam, M. Rashid, T. Chowdhury, M. Alam, Z. Alothman, K. Sopian, and N. Amin, Chalcogenide Lett. 11, 541 (2014).

[12] J. Yang, W. Yin, J. Park, J. Ma, and S. Wei, Semicond. Sci. Technol. 31, 22 (2016).

[13] J. Burst, J. Duenow, D. Albin, E. Colegrove, M. Reese, J. Aguiar, C. Jiang, M. Patel, M. Al-Jassim, D. Kuciauskas, S. Swain, T. Ablekim, K.G. Lynn, and W.Z. Metzger, Nat. Energy 1, 16015 (2016).

[14] I. Khan, V. Evani, V. Palekis, and C. Ferekides, IEEE J. Photovolt. 7, 1450 (2017)

[15] M. Sabighi, A. Majdabadi, S. Marjani, and S. Khosroabadi, Orient J. Chem. 31, 891 (2015).

[16] S. Khosroabadi and S. Keshmiri, in Proceedings of Iranian Conference on Electrical Engineering (2013), pp 1-4.

[17] A. Ojo and I. Dharmadasa, Sol. Energy 136, 10 (2016).

[18] M. McElroy, R. Page, D. Espinbarro-Valazquez, E. Lewis, S. Haigh, P. O'Brien, and D. Binks, , Thin Solid Films 560, 65 (2014)

[19] D. Kim, C. Hangarter, R. Debnath, J. Ha, C. Beauchamp, M. Widstrom, J. Guyer, N. Nguyen, B. Yoo, and D. Josell, Semicond. Sci. Technol. 109, 246 (2013).

[20] S. Tong , N. Mishra , C. Su , V. Nalla , W. Wu , W. Ji, J. Zhang, Y. Chan, and K. Loh, Adv. Funct. Mater. 24, 1904 (2014).

[21] W. Melvin, D. Kumar, and S. Devadason, Appl. Nanosci. 3, 453 (2013)

[22] C. Ferekides, D. Marinskiy, V. Viswanathan, B. Tetali, V. Palekis, P. Selvaraj and D. Morel, Thin Solid Films 361-362, 520 (2000).

[23] A. Salavei, D. Menossi, F. Piccinelli, A. Kumar, G. Mariotto, M. Barbato, M. Meneghini, G, Meneghesso, Si. Di Mare, E. Artegiani, and A. Romeo, Sol. Energy 139, 13 (2016).

[24] M. Reese, C. Perkins, J. Burst, S. Farrell, T. Barnes, S. Johnston, D. Kuciauskas, T. Gessert, and W. Metzger, J. Appl. Phys. 115305, 118 (2015).

[25] H. Ueng and S. Yang, J. Renew. Sustain. Ener. 011605, 4 (2012).

[26] S. Demtsu and J. Sites, in Proceedings of IEEE Photovoltaic Specialist Conference (2005), pp. 347-350.

[27] J. Sites, Sol. Energy Mater. Sol. Cells 75, 243 (2003).

[28] E. Cha, Y. Ko, S. Kim and B. Ahn, Curr. Appl. Phys. 17, 47 (2017).

[29] M. Zapata-Torres, J. Fernandez-Munoz, E. Hernandez-Rodriguez, R. Mis-Fernandez, V. Rejon, J. Pena, E. Valaguez-Velazquez, and A. Herrera, Superficies y Vacío. 28, 61 (2015).

[30] T. Liu, X. He, J. Zhang, L. Feng, L. Wu, W. Li, G. Zeng, and B. Li, J. Semicond. 33, 093003 (2012).

[31] M. Green, K. Emery, Y. Hishikawa, W. Warta and E. Dunlop, Prog. Photovolt. Res. Appl. 24, 905 (2016).

[32] C. Hernández-Vásquez, M. Albor-Aguilera, M. González-Trujillo, J. Flores-Márquez, D. Jiménez-Olarte, S. Gallardo-Hernández, and A. Orea, Mater. Res. Express 4 086403 (2017).

[33] X. Mathew, J. Drayton, V. Parikh, N. Mathews, X. Liu, and A. Compaan, Semicond. Sci. Technol. 24, 015012 (2009).

[34] S. Sordo, L. Abbene, E. Caroli, A. Mancini, A. Zappettini and P. Ubertini, Sensors, 9, 3491, (2009).

[35] X. Wu, R. Dhere, Y. Yan, I. Romero, Y. Zhang, J. Zhou, C. Dehart, A. Duba, C. Perkins, and B. To, in Proceedings of IEEE Photovoltaic Specialist Conference (2002), pp. 531–534.

[36] D. Meysing, M. Griffith, W. Rance, M. Reese, J. Burst, C. Wolden, and T. Barnes, in Proceedings of IEEE Photovoltaic Specialist Conference (2014), pp. 964–967.

[37] D. Duncan, J. Kephart, K. Horsley, M. Blum, M. Mezher, L. Weinhardt, M. Haming, R. Wilks, T. Hofmann, W. Yang, M. Bar, W. Sampath, and C. Heske, ACS Appl. Mater. Interfaces 7, 16382 (2015).

[38] J. Kephart, R. Geisthardt, and W. Sampath, Prog. Photovolt. Res. Appl. 123, 1484 (2015).

[39] T. Minemoto, Y. Hashimoto, T. Satoh, T. Negami, H. Takakura, and Y. Hamakawa, J. Appl. Phys. 89, 8327 (2001).

[40] C. Niedermeier, M. Råsander, S. Rhode, V. Kachkanov, B. Zou, N. Alford, and M. Moram, Sci. Rep. 6, 31230 (2016)

[41] S. Heo, E. Cho, H. Lee, G. Park, H. Kang, T. Nagatomi, P. Choi, and B. Choi, AIP Adv. 5, 077167 (2015).

[42] T. Maemoto, N. Ichiba, H. Ishii, S. Sasa, and M. Inoue, J. Phys. Conf. Ser. 59, 670 (2007).

[43] M. Lorenz, E. Kaidashev, H. Wenckstern, V. Riede, C. Bundesmann, D. Spemann, G. Benndorf, H. Hochmuth, A. Rahm, H. Semmelhack, and M. Grundmann, Solid State Electron. 47, 2205 (2003).

[44] J. Li, X. Li, Y. Yan, C. Jiang, W. Metzger, I. Repins, M. Contreras, and D. Levi, J. Vac. Sci. Technol. B27, 2384 (2009).

[45] J. Sites, A. Munshi, J. Kephart. D. Swanson, and W. Sampath, in Proceedings of IEEE Photovoltaic Specialist Conference (2016), pp. 3632–3635.

[46] T. Song, A. Moore, and J. Sites, IEEE J. Photovolt. 99, (2017).

[47] J. Kephart, J. McCamy, Z. Ma, A. Ganjoo, F. Alamgir, and W. Sampath, Sol. Energy Mater. Sol. Cells, 157, 266 (2016).

[48] A. Delahoy, X. Tan, A. Saraf, P. Patra, S. Manda, Y. Chen, K. Velappan, B. Siepchen, S. Peng, and K. Chin, in Proceedings of IEEE Photovoltaic Specialist Conference (2017).

[49] J. Kephart, R. Geisthardt, and S. Sampath, in Proceedings of IEEE Photovoltaic Specialist Conference (2011), pp. 854-858.

[50] J. Kephart, and M. Sampath, in Proceedings of IEEE Photovoltaic Specialist Conference (2015), pp. 1-4.

[51] T. Minemoto, T. Matsui, H. Takakura, Y. Hamakawa, T. Negami, Y. Hashimoto, T. Uenoyama, and M. Kitagawa, Sol. Energy Mater. Sol. Cells 67, 83 (2001).

[52] Y. Chen, S. Peng, X. Tan, X. Cao, B. Siepchen, G. Fu, A. Delahoy, and K. Chin, in Proceedings of IEEE Photovoltaic Specialist Conference (2016), pp. 424–427.

[53] Y. Chen, X. Tan, S. Peng, C. Xin, A. Delahoy, K. Chin, and C. Zhang, J. Electron. Mater. (2017), https://doi.org/10.1007/s11664-017-5850-9.

[54] J. Granata, J. Sites, G. Contreras-Puente, and A. Compaan, in Proceedings of IEEE Photovoltaic Specialist Conference (1996), pp. 854-856.

[55] K. Nakamura, M. Gotoh, T. Fujihara, T. Toyama, and H. Okamoto, Sol. Energy Mater. Sol. Cells, 75, 185 (2003).

[56] Y. Chen, S. Peng, X. Cao, A. Delahoy, and K. Chin, in Proceedings of IEEE Photovoltaic Specialist Conference (2017).

[57] S. Peng, Xin Cao, J. Pan, X. Wang, X. Tan, A. Delahoy and K. Chin, J. Electron. Mater. 46, 1405, (2017).

[58] T. Minami, Semicond. Sci. Technol. 20, S35 (2005).

[59] T. Tsai and Y. Wu, Microelectron. Eng. 83, 536 (2006).

[60] G. Agostinelli, D. Ba¨tzner, and M. Burgelman, in Proceedings of IEEE Photovoltaic Specialist Conference (2002), pp. 744–747.

[61] Y. Inoue, M. Ha´la, A. Steigert, R. Klenk, and S. Siebentritt, in Proceedings of IEEE Photovoltaic Specialist Conference (2015), pp. 1–5.

[62] K. Saeed and H. Seyyed, Opt. Express 22, A921 (2014).

[63] J. Verschraegen and M. Burgelman, Thin Solid Films 515, 6276 (2007).

[64] J. Tauc, Mater. Res. Bull. 3, 37 (1968).

[65] K. Chin, J. Appl. Phys. 111, 104509 (2012).

[66] K. Chin, J. Semicond. 34, 122001 (2013).

[67] K. Chin and Z. Cheng, J. Semicond. 37, 092003 (2016).

[68] W. Shockley and W. Read, Phys. Rev. 87, 835 (1952).

[69] Z. Zekry and G. Eldallal, Solid State Electron. 31, 91 (1988).

[70] A. Delahoy, S. Peng, P. Patra, S. Manda, A. Saraf, Y. Chen, X. Tan, and K. Chin, in Proceedings of MRS Advances (2017), pp 1-12.

[71] Z. Wang, Z. Cheng, A. Delahoy, and K. Chin, IEEE J. Photovolt. 3, 843 (2013).

[72] A. Delahoy, Z. Cheng, and K. Chin, EU Photovoltaic Specialist Conference (2012), pp. 2837-2842.

[73] R. Dhere, Y. Zhang, M. Romero, S. Asher, M. Young, B. To, R. Noufi, and T. Gessert, in Proceedings of IEEE Photovoltaic Specialist Conference (2008), pp. 1–5.

[74] I. Visoly-Fisher, S. Cohen, and D. Cahen, Appl. Phys. Lett. 82, 556 (2003).

[75] A. Delahoy and S. Guo, Handbook of Photovoltaic Science and Engineering, ed. A. Luque and S. Hegedus: Wiley, pp 716-796 (2011).

[76] R. Shao, M. Gloeckler, and B. Buller, US2012/0067422 A1, Patent, 2012.